

## **Todo list**



## AIX-MARSEILLE UNIVERSITY

### DOCTORAL SCHOOL: Physics and Material Science

PARTENAIRES DE RECHERCHE

Laboratoire MADIREL

Submitted with the view of obtaining the degree of doctor

Discipline: Material Science

Specialty: Characterisation of porous materials

**Paul Iacomi**

Exploring sources of variability in metal organic frameworks through high  
throughput adsorption and calorimetric methods

Defended on 15/10/2018 in front of the following jury:

Rob Ameloot	KU Leuven	Rapporteur
Flor Siperstein	The University of Manchester	Rapporteur
Stefan Kaskel	TU Dresden	Examinateur
Jeff Kenvin	Micromeritics Inc.	Examinateur
Philip L. Llewellyn	CNRS/AMU	Directeur de thèse

National thesis number: 2017AIXM0001/001ED62



This work falls under the conditions of the Creative Commons Attribution License - No commercial use - No modification 4.0 International.

# Abstract

Metal-organic frameworks (MOF) are a class of hybrid porous materials which has been the focus of much scientific interest since their discovery in the late 20<sup>th</sup> century. These coordination polymers consist of three-dimensional networks of metal nodes interlinked by polytopic organic molecules. The interest in these materials stems from the possible rational design of MOFs for highly efficient or unique applications. With judicious choice of building blocks, the framework can be used for carbon dioxide capture from air, hydrogen storage or regioselective catalysis. Taking advantage of specific properties of porous coordination polymers such as flexibility, magnetism or photovoltaics may even result in their use in drug delivery, micro mechanical devices, sensors or optoelectronics.

However, their unique properties also introduce significant difficulty in MOF characterisation through gas adsorption. Structural defects, crystal size, shaping procedure and the aforementioned flexible behaviour can lead to variability in adsorption results. In this thesis large scale processing of isotherms is first used to explore the scale of uncertainty present in porous material adsorption data. The high throughput methodology is then extended through the use of *in situ* calorimetry as an avenue to gain further insight into the contribution of material, guest-host and host-host interactions to the overall energetics of adsorption. Together, these two methods can be used to quantify the effect of structural defects in MOFs, material shaping with different binders and even yield fundamental know-how of how adsorption induces compliance in flexible materials.

# Résumé

Les réseaux métallo-organiques (MOF) sont une classe de matériaux poreux hybrides qui ont suscité un grand intérêt scientifique depuis leur découverte à la fin du 20ème siècle. Ces polymères de coordination sont constitués de réseaux tridimensionnels de nœuds métalliques interconnectés par des molécules organiques polytopiques. L'intérêt pour ces matériaux provient de la conception rationnelle possible des MOF pour des applications hautement efficaces ou uniques. Avec un choix judicieux des blocs de construction, le cadre peut être utilisé pour la capture du dioxyde de carbone dans l'air, le stockage de l'hydrogène ou la catalyse régiosélective. Tirer parti des propriétés spécifiques des polymères de coordination poreux tels que la flexibilité, le magnétisme ou la photoélectrique peut même conduire à leur utilisation dans la délivrance de médicaments, des dispositifs micro-mécaniques, des capteurs ou en optoélectronique.

Cependant, leurs propriétés uniques introduisent également des difficultés importantes dans la caractérisation des MOF par adsorption de gaz. Les défauts structurels, la taille des cristaux, la procédure de mise en forme et le comportement flexible susmentionné peuvent entraîner une variabilité des résultats de l'adsorption. Dans cette thèse, le traitement à grande échelle des isothermes est d'abord utilisé pour explorer l'échelle d'incertitude présente dans les données d'adsorption des matériaux poreux. La méthodologie à haut débit est ensuite étendue à l'utilisation de la calorimétrie *in situ* comme moyen de mieux comprendre la contribution des interactions matériau-matériau, matériau-hôte et hôte-hôte à l'énergie globale de l'adsorption. Ensemble, ces deux méthodes peuvent être utilisées pour quantifier l'effet des défauts structurels dans les MOF, la mise en forme des matériaux avec différents liants et même un savoir-faire fondamental sur la manière dont l'adsorption induit la conformité dans les matériaux flexibles.

# **Acknowledgements**

# Contents

<b>Abstract</b>	<b>iii</b>
<b>Résumé</b>	<b>iv</b>
<b>Acknowledgements</b>	<b>v</b>
<b>Introduction to this thesis</b>	<b>1</b>
<b>1 Building a framework for isotherm data processing</b>	<b>2</b>
1.1 Introduction . . . . .	2
1.2 Physical models of adsorption . . . . .	3
1.2.1 The Gibbs surface excess approach . . . . .	6
1.2.2 The Henry model . . . . .	7
1.2.3 Langmuir and multi-site Langmuir model . . . . .	7
1.2.4 The Brunauer-Emmett-Teller model . . . . .	9
1.2.5 Toth model . . . . .	10
1.2.6 Temkin model . . . . .	11
1.2.7 Jensen-Seaton model . . . . .	11
1.2.8 Quadratic model . . . . .	11
1.2.9 Virial model . . . . .	12
1.2.10 Vacancy solution theory models . . . . .	12
1.3 Characterisation of materials through adsorption . . . . .	13
1.3.1 Specific surface area and pore volume calculation . . . . .	14
1.3.2 Assessing porosity . . . . .	17
1.3.3 Predicting multicomponent adsorption . . . . .	22
1.4 pyGAPS overview . . . . .	24
1.4.1 Core structure . . . . .	24
1.4.2 Creation of an Isotherm . . . . .	26
1.4.3 Units . . . . .	28
1.4.4 Workflow . . . . .	28
1.4.5 Characterisation using pyGAPS . . . . .	29
1.5 Processing a large adsorption dataset . . . . .	37
1.5.1 The NIST ISODB dataset . . . . .	37
1.5.2 A comparison between surface area calculation methods . . . . .	38

---

1.5.3 Variability of the dataset . . . . .	39
1.6 Conclusion . . . . .	42
Bibliography . . . . .	43
<b>2 Extending analysis of porous compounds through calorimetry</b> . . . . .	<b>46</b>
2.1 Introduction . . . . .	46
2.2 Energetics of adsorption . . . . .	47
2.2.1 Forces involved in adsorption . . . . .	47
2.2.2 Thermodynamic quantities of the adsorbed phase . . . . .	48
2.2.3 Application of differential enthalpy of adsorption to the characterisation of materials . . . . .	49
2.3 Measuring the enthalpy of adsorption . . . . .	50
2.3.1 Isosteric enthalpy of adsorption . . . . .	50
2.3.2 Microcalorimetry . . . . .	51
2.3.3 Experimental apparatus and accuracy . . . . .	54
2.4 Case studies for the use of microcalorimetry combined with adsorption experiments . . . . .	55
2.4.1 Comparison between enthalpies of adsorption measured through the direct and indirect method . . . . .	55
2.4.2 An example dataset on a reference material . . . . .	56
2.4.3 A study on a novel MOF . . . . .	58
2.5 Conclusion . . . . .	62
Bibliography . . . . .	63
<b>3 Exploring the impact of structural defects—post-synthesis generation of missing linkers in UiO-66(Zr)</b> . . . . .	<b>66</b>
3.1 Introduction . . . . .	66
3.2 The defective nature of MOFs . . . . .	68
3.2.1 Types of crystal defects and their analogues in MOFs . . . . .	68
3.2.2 Consequences of defects . . . . .	70
3.2.3 Defect engineering of MOFs . . . . .	71
3.2.4 The propensity of UiO-66(Zr) for defect generation . . . . .	72
3.3 Materials and methods . . . . .	73
3.3.1 Materials . . . . .	73
3.3.2 Methods for quantifying defects . . . . .	74
3.4 Results and discussion . . . . .	76
3.4.1 Crystallinity of leached samples . . . . .	76
3.4.2 Thermogravimetry results . . . . .	76
3.4.3 Nitrogen sorption at 77K . . . . .	79
3.4.4 Characterisation of trends . . . . .	81

---

---

3.4.5 Carbon dioxide isotherms . . . . .	86
3.5 Conclusion . . . . .	88
Bibliography . . . . .	89
<b>4 Exploring the impact of material shaping — wet granulation of stable MOFs</b>	<b>94</b>
4.1 Introduction . . . . .	94
4.2 Shaping in context . . . . .	95
4.3 Materials, shaping and characterisation methods . . . . .	97
4.3.1 Materials . . . . .	97
4.3.2 Shaping Procedure . . . . .	99
4.3.3 Characterisation of powders and pellets . . . . .	99
4.3.4 Sample activation for adsorption . . . . .	99
4.4 Results and discussion . . . . .	100
4.4.1 Thermal stability . . . . .	100
4.4.2 Adsorption isotherms at 77K and room temperature . . . . .	100
4.4.3 Room temperature gas adsorption and microcalorimetry . . . . .	103
4.4.4 Vapour adsorption . . . . .	109
4.5 Conclusion . . . . .	115
Bibliography . . . . .	117
<b>5 Exploring intrinsic framework phenomena — adsorption induced phase changes</b>	<b>119</b>
5.1 Introduction . . . . .	119
5.2 Compliance in porous crystals . . . . .	120
5.2.1 Examining the assumption of a rigid adsorbent . . . . .	120
5.2.2 Flexibility in metal organic frameworks . . . . .	121
5.2.3 Describing and inducing MOF compliance . . . . .	123
5.2.4 Consequences and applications of flexible MOFs . . . . .	124
5.2.5 Unique flexible behaviour of DUT-49 . . . . .	125
5.3 Materials and characterisation methods . . . . .	126
5.3.1 Materials . . . . .	126
5.3.2 Characterisation methods . . . . .	127
5.4 Results and discussion . . . . .	130
5.4.1 The structural transition leading to NGA in DUT-49 . . . . .	130
5.4.2 Impact of framework structure on transition mechanics . . . . .	133
5.4.3 An in-depth analysis of the NGA mechanism . . . . .	140
5.5 Conclusion . . . . .	151
<b>Conclusion and outlook</b>	<b>159</b>
<b>A Common characterisation techniques</b>	<b>160</b>
A.1 Thermogravimetry . . . . .	160

---

A.2 Bulk density determination . . . . .	160
A.3 Skeletal density determination . . . . .	161
A.4 Nitrogen physisorption at 77 K . . . . .	161
A.5 Vapour physisorption at 298 K . . . . .	161
A.6 Gravimetric isotherms . . . . .	162
A.7 High throughput isotherm measuremnt . . . . .	162
A.8 Powder X-ray diffraction . . . . .	162
A.9 Nuclear magnetic resonance . . . . .	162
A.10 Adsorption manometry and calorimetry at 303 K . . . . .	162
Bibliography . . . . .	162
<b>B Synthesis method of referenced materials</b>	<b>163</b>
B.1 Takeda 5A reference carbon . . . . .	163
B.2 MCM-41 mesoporous silica . . . . .	163
B.3 Zr fumarate MOF . . . . .	163
B.4 UiO-66(Zr) for defect study . . . . .	164
B.5 UiO-66(Zr) for shaping study . . . . .	164
B.6 MIL-100(Fe) for shaping study . . . . .	164
B.7 MIL-127(Fe) for shaping study . . . . .	165
Bibliography . . . . .	165
<b>C Calculation of uncertainty in adsorption measurements</b>	<b>166</b>
Bibliography . . . . .	166
<b>D Appendix for chapter 2</b>	<b>167</b>
D.1 Propane/propylane isotherms . . . . .	167
D.2 TGA curves . . . . .	168
D.3 Water isotherms . . . . .	168
Bibliography . . . . .	169
<b>E Appendix for chapter 3</b>	<b>170</b>
E.1 Acid and solvent properties . . . . .	170
E.2 Powder diffraction patterns . . . . .	171
E.3 TGA curves . . . . .	172
E.3.1 DMF leached samples . . . . .	172
E.3.2 Water leached samples . . . . .	173
E.3.3 Methanol leached samples . . . . .	174
E.3.4 DMSO leached samples . . . . .	175
E.3.5 High resolution curves . . . . .	176
E.4 Nitrogen sorption isotherms . . . . .	177
E.4.1 DMF leached samples . . . . .	177

E.4.2 H <sub>2</sub> O leached samples . . . . .	178
E.4.3 MeOH leached samples . . . . .	180
E.4.4 DMSO leached samples . . . . .	182
E.5 Characterisation . . . . .	184
Bibliography . . . . .	184
<b>F Appendix for chapter 4</b>	<b>185</b>
F1 Calorimetry dataset UiO-66(Zr) . . . . .	186
F2 Calorimetry MIL-100(Fe) . . . . .	188
F3 Calorimetry MIL-127(Fe) . . . . .	190
<b>G Appendix for chapter 5</b>	<b>192</b>
G.1 Table of properties for low temperature probes . . . . .	192
G.2 Ambient temperature calorimetry experiments . . . . .	193
G.3 Low temperature calorimetry experiments . . . . .	197

# **5 Exploring intrinsic framework phenomena — adsorption induced phase changes**

## **5.1 Introduction**

Until this chapter, it has been assumed that the porous materials remain rigid when adsorbing a gas. Differences in pore size, crystallinity or structure may exist, but these properties are assumed not to change as the host fluid enters the pores. In most cases this is a reasonable supposition. However, it is not universally applicable, as the forces and interactions exerted during adsorption may induce changes in solid itself.

Such effects in classic porous inorganic materials like zeolites, carbons and clays take the form of structural contraction and expansion, swelling or counterion displacement.<sup>(?)</sup> It is only recently that flexibility was discovered in coordination polymers, such as MOFs. A feature which arises from their comparatively weak coordination bonds or pliant organic components, it allows for a systematic deflection of bonds throughout the entire crystal lattice. As such, the term “soft porous crystal” defines porous solids that are both highly ordered and possess the ability to reversibly transform their structure upon external stimuli. Part of the so-called third generation of crystalline porous compounds, they represent some of the latest developments in the field of MOFs.

The unique properties of flexible materials can preclude their application in fields such as sensing, micromechanical devices and highly efficient gas storage. It is these perspectives that make their synthesis and design a key research interest. However, their flexible nature introduces new challenges in their characterisation, as factors such as temperature and thermal history<sup>(?)</sup>, crystal size<sup>(?)</sup>, external pressure<sup>(?)</sup>, structural defects<sup>(?)</sup> and even adsorption kinetics play a role in their compliance. This type of variability goes beyond what has been insofar discussed in this thesis and it is here where a combined characterisation approach becomes essential in understanding the fundamental physics governing flexibility and prediction of adsorption behaviour. In this chapter, a study of the differential enthalpy of adsorption on DUT-49, a soft coordination polymer, measured directly through calorimetric methods as detailed in chapter 2, will be seen to shed light on the source of flexibility and the effectiveness of different avenues for its control.

## Summary

After a brief introduction of the background of soft porous materials, this chapter will present the characterization of a novel flexible MOF (DUT-49) and its analogues. This material undergoes a sudden contraction of its unit cell into a lower volume state upon adsorption, resulting in the expulsion of gas from its pores. This phenomena was coined “negative gas adsorption” (NGA). The text will focus on characterisation through calorimetric methods performed by Paul Iacomi, together with references of results obtained by collaborating groups, included in order obtain a complete story of the underlying mechanism behind NGA.

## Contribution

The synthesis of all MOFs was performed by Simon Krause (TU Dresden), as well as the adsorption of multiple probes and the neutron diffraction study. Ambient and low temperature calorimetry was carried out by Paul Iacomi. Computer simulations of adsorption isotherms, linker buckling and structural contraction are the result of work from Jack Evans and Dr. FX Coudert. Mechanical compression experiments were performed in the group of Prof. Guillaume Maurin in Montpellier. Dr. Philip Llewellyn and Prof. Stefan Kaskel were instrumental in the interpretation of the results obtained.

## 5.2 Compliance in porous crystals

### 5.2.1 Examining the assumption of a rigid adsorbent

Adsorption induced changes in porous media have been known to occur for over 90 years<sup>(?)</sup>, with clays, coals and polymers undergoing swelling during gas or vapour uptake.<sup>(?)</sup> However, the effect upon the macroscopic properties of the material is often negligibly small and of little consequence to industrial adsorption processes. Studies of this aspect of porous adsorbents have therefore been scarce in the large part of the 20<sup>th</sup> century, likewise influenced by lack of sufficiently accurate methods for characterising and modelling such occurrences.

In recent years, the advent of reference materials, highly sensitive methods such as synchrotron grade light sources and *in silico* computational techniques such as DFT has put at our disposal the tools required to study these transformations. Together with the discovery of their role in natural and industrial processes e.g. the swelling of shale during natural gas extraction, maturation of concrete and the perspectives afforded by novel porous materials, these factors have generated much scientific interest in material compliance. As an example, the attractive option of combined carbon capture and methane recovery implemented through pumping of carbon dioxide into reservoirs is prohibited by swelling-induced loss of porosity and well blocking.<sup>(?)</sup>

In-depth studies<sup>(?)</sup> have revealed that most porous materials possess some small degree of compliance, with *in-situ* dilatometry going so far as to obtain pore size distributions from accurate volume changes.<sup>(?)</sup> Most flexible processes can be likened to continuous order transitions. It is, however, the discovery of large scale flexibility in MOFs such as MIL-53 and linker-controlled gate opening like in ZIF-8, where the transformation between the different framework states occurs suddenly at precise points in the loading curve, which has shown that compliance may also take the form of a first-order transition. Such types of transformations are desirable<sup>(?)</sup> due to their highly specific response. The possible dependence of flexibility on other stimuli, such as light, mechanical pressure, temperature or magnetic fields may allow for precise tuning of structural changes. As such, it is reasonable to state that the flexible nature of the solid phase can no longer be ignored.

### 5.2.2 Flexibility in metal organic frameworks

Since the highlight of compliance in porous coordination polymers in the report of<sup>(?)</sup>, much progress has been made in the synthesis and understanding of this phenomenon. An exhaustive review of MOF flexibility is outside the scope of this thesis, with the field progressing rapidly enough to generate a wealth of critical literature.<sup>(???????)</sup> Some of the known types of structural flexibility encountered in MOFs will be briefly discussed, with a summary available in Figure 5.1.

Since MOFs, like clays and graphite, can form discrete two-dimensional sheets, bound together by weak Van-der-Waals,  $\pi - \pi$  interactions or hydrogen bonds, adsorbed molecules may force these layers apart by intercalation. The concept is taken further in the pillared layer approach, where the sheets are connected by tertiary linkers instead of weak attractions. These can act as springs, allowing pore expansion while maintaining structural integrity.

As briefly mentioned in chapter 3, a large void space in the unit cells allows secondary networks to grow throughout the MOF, effectively creating an intercalated structure.<sup>(??)</sup> These secondary grids are independent of the primary framework and are displaced upon guest adsorption.<sup>(?)</sup> This internal translation may also be associated with a tilting of the linker<sup>(?)</sup>, combining intercalation with structural-deformation type flexibility.

The origin of flexibility may be purely due to the linker itself. Organic bonds are inherently labile, as seen in polymer chains, since unsaturated connections in the linker may bend if the strain on the organic strut overcomes its tensile strength. Increasing the linker length often induces this type of flexibility, for example in the IRMOF isoreticular series of materials.<sup>(?)</sup> Even an unsaturated bond may be induced by a photon with a suitable energy to undergo an analogue of a *cis-trans* transition. The deformation may also lead to expansion and therefore of framework swelling, as encountered in MIL-88 and its derivatives.<sup>(?)</sup>

MOFs can also have structural flexibility which does not require any volume changes in

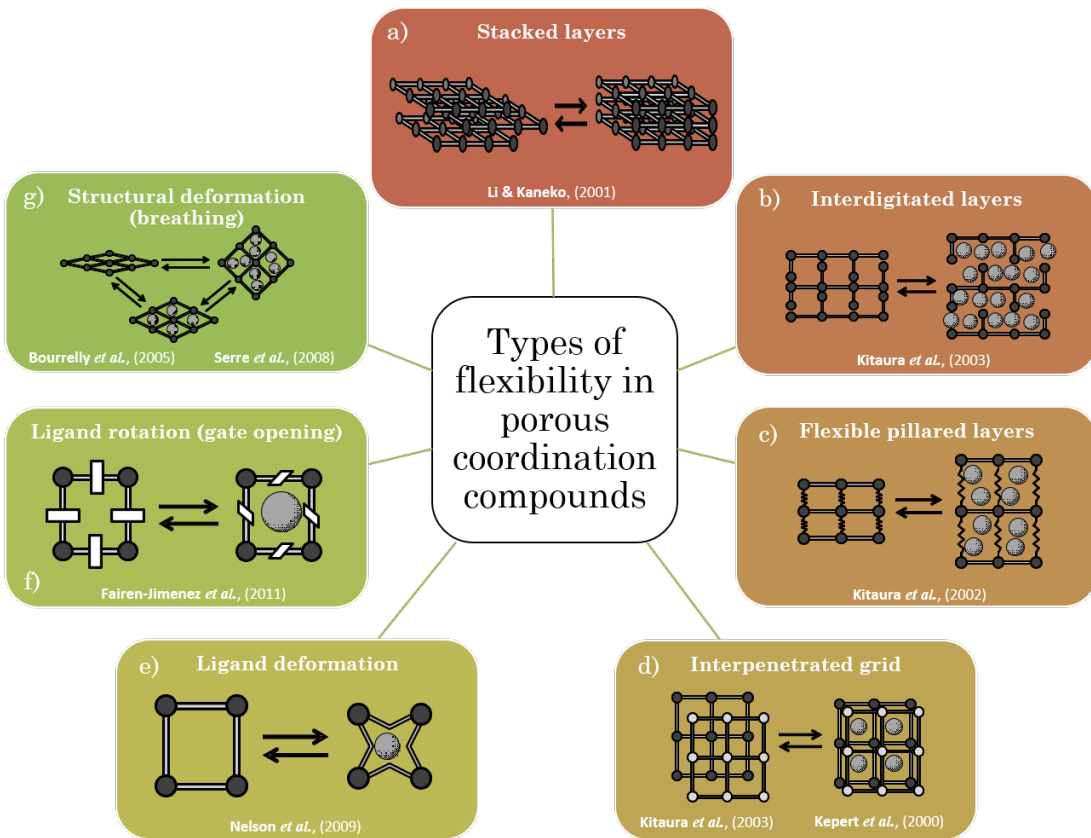


**Figure 5.1:** A (non-exhaustive) visual summary of the types of flexibility documented in MOFs, as detailed in (a) <sup>?</sup> (b) <sup>?</sup> (c) <sup>?</sup> (d) <sup>?, ?</sup> (e) <sup>?</sup> (f) <sup>?</sup> (g) <sup>?, ?, ?</sup>

the unit cell. The rotation of linkers can act as gateing for different guests, allowing entry of probes larger than the window size would suggest or preferential adsorption of a gas which has the right property to act as a “key” from a mixture.<sup>(?)</sup> The former effect is common in zeolithic imidazole frameworks (ZIFs).<sup>(?)</sup>

The discovery of the so-called “breathing” type of structural deformation<sup>(?, ?, ?)</sup> in the MIL-53 and MIL-47 family of materials has revealed step-like transformations in its unit cell size and metastable intermediaries with an open pore (*op*), closed pore (*cp*) and narrow/intermediate states (*np*/*ip*). No other family of flexible MOFs has, to date, generated more scientific interest. This is likely due to the relative stability of the material, combined with its ability to undergo massive and reversible structural deflections, while retaining its crystallinity. The relatively simple structure and large capability for functionalisation, either through ligand modification or exchange of the metal node (with variants of MIL-53 synthesised for Cr, Fe, Al, Sc, Ga or In), allowed for its use as an archetypal material for the study of flexible behaviour. More recently, similar materials, like DUT-8(M) (M=Ni, Co, Cu, Zn) which allow the impact of the metal<sup>(?)</sup> on compliance to be evidenced have emerged.

### 5.2.3 Describing and inducing MOF compliance

The mechanistic phenomena during adsorption can be seen as an overlap<sup>(?)</sup> of several competing effects: a sub-monolayer contraction<sup>(?)</sup> resulting from micropore bridging or surface stresses, followed by a monotonic expansion with the gradual decrease of the solid-fluid interface energy also known as the Bangham effect.<sup>(?)</sup> Such behaviour is highly dependent of pore size, geometry and anisotropy, with condensation in macropores a further complex source of strain.<sup>(???)</sup> The degree of adsorption induced changes in a framework is generally a function of its porosity, with very high surface area materials such as aerogels capable of undergoing up to 30% deformation.<sup>(?)</sup> In MOFs, the adsorption stresses are no different than in other materials. However, the ability of the porous network to undergo displacements is much higher, since its rigidity is in between that of “hard” adsorbents such as zeolites/silica and “soft” organic polymers (although porous covalent frameworks can also achieve self-support and porosity).

Finding a suitable model that would predict both the adsorption induced stress and the resulting structural changes from strain has so far remained a challenge. A thermodynamic-based method which has been successfully applied to breathing MOFs is that of <sup>(?)</sup>. This model assumes that the deformation strain is fully determined due to surface stress, calculated from the grand thermodynamical potential of a rigid analogue of the pore. It has been used to explain the existence domains of MIL-53(Al)<sup>(?)</sup>, in conjunction with an osmotic thermodynamic description of the framework itself.<sup>(?)</sup> For mesoporous materials, the stress-strain model has been extended by <sup>(?)</sup> through the Derjaguin–Broekhoff–de Boer (DBdB) theory<sup>(?)</sup> and applied to predict the resulting strain in mesoporous silica. Nevertheless a complete theory of adsorption-deformation which can fully predict the changes in the measured enthalpy of adsorption and the mechanistic behaviour of MOFs has remained elusive.

The most promising characteristics of flexible MOFs are the ability to control the compliance through external means which are detached from guest loading, that would dramatically expand their potential applications. Pure mechanical pressure on a flexible material is often enough to induce transitions. First observed on ZIFs, through pressure induced phase change<sup>(??)</sup> and latter applied to breathing MOFs using mercury porosimetry<sup>(??)</sup>, it shows a direct relationship between the bulk modulus of a MOF and its flexible behaviour. Entropic control through temperature-induced switching has been shown to be possible in MIL-53 by <sup>(?)</sup>, explained as a change in the range of metastability of its pore forms.<sup>(?)</sup> More precise external control may be possible if molecules which have the ability to switch their state when exposed to suitable wavelengths are used as linkers. In this case light irradiation may be used to force the transition.<sup>(?)</sup> Magnetic field dependent switching can also be theorised, although has not been so far encountered. One of the least understood factors that changes the flexible behaviour of porous crystals is the effect of particle size. It is clear that the thermodynamical potential of the crystal surface has a profound influence on its compliance, as shown

on the large shift of the gate-opening pressure of ZIF-8.<sup>(?)</sup> However, a rigorous model of the contribution of the surface on breathing has yet to be developed in our knowledge. Finally, the presence of structural defects likely impacts the framework flexibility, as highlighted by <sup>(?)</sup> in a recent article, although currently few studies have focused on this subject.

#### 5.2.4 Consequences and applications of flexible MOFs

The study of flexible MOFs is motivated from both a desire for the fundamental understanding of compliance and from the potential applications of such systems. The use of soft porous crystals in sensing and gas storage and separation is evident, although applications in catalysis, electrochemistry and drug delivery have also been alluded to by recent studies.

The usefulness of adsorption induced flexibility for sensors or actuators has been recognised, initially by nature itself, with humidity induced swelling acting to open pine cones.<sup>(?)</sup> More recently, similar sensing devices based on adsorption strain in mesoporous silica have been developed such as a flexing silica-polymer membrane<sup>(?)</sup> or deformation of a nano sized cantilever<sup>(?)</sup> which show promise for use in micromechanical systems.

From a gas storage and separation point of view, changes in the adsorbent structure may yield crucial process improvements. Pressure swing adsorption (PSA) is heavily dependent on the working capacity of the adsorbent used, or the difference between loading at the operation pressure and at the regeneration pressure. In this case, an S-shaped isotherm, with the vertical part of the slope in the aforementioned pressure range would lead to high process efficiency gains by eliminating material “dead volume adsorbed”.<sup>(?)</sup> In a temperature swing process (TSA), where the regeneration is performed through heating of the adsorbent bed, the key parameter is the integral enthalpy of adsorption, a measure of the energy requirements for the process. As a part of the chemical potential of the adsorbed phase is used by the mechanical contraction of the material, flexible adsorbents have the advantage of intrinsic thermal management, reducing the energy cost.<sup>(?)</sup> Both effects are equally applicable to the storage of pure gasses, increasing the storage capacity and minimizing the energetic requirement of recovery. Entrapment of guest molecules inside a gated pore might lend itself to temperature controlled storage and release of gasses<sup>(?)</sup>, or “sealing” of a target gas inside the structure once adsorption has taken place. It is also possible that by using external mechanical pressure to control flexibility, the adsorption behaviour of porous materials may be tuned, as suggested by the work of <sup>(?)</sup> on MIL-53.

Catalytic applications of flexible MOFs could be envisaged where the switching behaviour can bring into contact active sites or hold reactants in place until complete reaction has taken place. A recent study by <sup>(?)</sup>, has shown that the redox potential of the sulphur bond in a tetrathiafulvalene breathing MOF is dependent on its dihedral angle in different pore states. This raises the possibility of tunability of the oxidation potential of flexible framework. Fi-

nally flexible MOFs constructed of biocompatible materials could be used as drug delivery methods<sup>(??)</sup> if release of the encapsulated molecule is triggered through a structural transition.

### 5.2.5 Unique flexible behaviour of DUT-49

It is clear that one of the most desirable kinds of flexibility is one that can be likened to a Heaviside step function, where switching occurs between two or more material states at a well defined pressure. However, not many MOFs synthesised to date follow this type of behaviour. It is why the surprising compliance of DUT-49, a highly porous structure, has generated interest in the MOF community.

In the initial paper of <sup>?</sup>, the synthesis of DUT-49 through a super-molecular approach is described, with the goal of generating a highly porous material. The MOF is built through the secondary building unit (SBU) approach, where the crystallographic vertices of the structure are metal organic polyhedra (MOP), in this case 12-connected cuboctahedra based on copper paddlewheels, which are then connected by a tetratopic carboxilate linker. The resulting MOF forms a face centered cubic (**fcu**) net if the MOP are considered as nodes and a trimodal pore size distribution: the 1.2 nm MOP, a 1.8 nm tetrahedron and a very large 2.6 nm octahedron. The material has a high nitrogen accessible surface area (of more than  $5000 \text{ m}^2/\text{g}$ ) and accessible volume (84.7%).

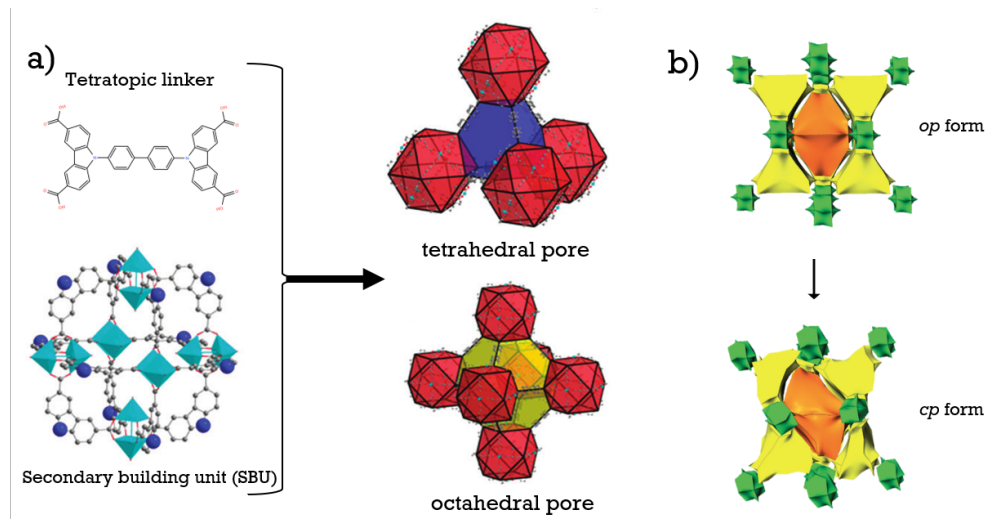


**Figure 5.2:** (a) The tetratopic linker and secondary copper paddlewheel building unit used to synthesise DUT-49, and the resulting structure and generated pores.<sup>(?)</sup> (b) Two possible phases of the material, with the open to closed pore transition.<sup>(?)</sup>

In the original study, the MOF did not show any flexible behaviour. However, it was later found by <sup>?</sup> that when adsorbing  $\text{CH}_4$  at 111 K, a sharp step occurs in the isotherm, accompanied by a decrease in unit cell volume. This step corresponds to a reduction in the pore size

of the MOF, transforming the *open pore (op) form* in a *contracted (cp) form*, also referred to as a *closed pore phase* (a term used even if this form still has a large accessible void space). More interestingly, the process is accompanied by an expulsion of the adsorbed gas from the interior of the pores, increasing the pressure in the experiment cell. This type of pressure-amplifying transition has been coined negative gas adsorption (NGA) and was found to occur with other adsorbates at different temperatures such as C<sub>4</sub>H<sub>10</sub> at 303 K or Xe at 195 K, which allowed study of the transition at ambient temperature and through <sup>129</sup>Xe NMR spectroscopy.<sup>(?)</sup>

The origin of this phenomenon has been elucidated by <sup>(?)</sup> where it has been shown to emerge due to a buckling of the central strut of the tetratopic linker under compressive stress induced by adsorption, similar to the failure of a metal column under critical load. The *op* and *cp* phase stability depends on the adsorbate loading of the material, with the *op* form being energetically favoured at zero and high loadings. At intermediate pore filling, the *cp* state is stabilized by the fluid molecules and becomes energetically favoured. At this point, the *op* phase enters a metastable regime and can contract if the energy barrier between the two states is overcome. As the transition from the *cp* to the *op* state requires an activation energy, re-opening of the structure is only possible through complete structure loading. If the system is in its *cp* state during adsorbate removal, the structure undergoes structural collapse, attaining an amorphous state. The MOP are still available for adsorption in this state, as the resulting material can be observed to be microporous in nature but without a well defined structure.

However, questions still remain about the driving forces behind the transition itself, such as the contribution of guest-host interactions, as well as the temperature range and adsorbates where it is possible. The rational design of such materials is also put into question, where framework parameters such as linker length, functionalisation and composition may be used to tune the pressure and extent of NGA. It is here where the adsorption methodology introduced in chapter 1 combined with *in-situ* calorimetry as presented in chapter 2 can be used to shed light on the energetic background of NGA in DUT-49.

## 5.3 Materials and characterisation methods

### 5.3.1 Materials

Several DUT materials have been synthesised in order to study the effect of different parameters on the switching behaviour. From the point of view of the criterion of interest, the materials can be divided into the several categories. The material name, together with the central part of the linker, which was modified to change the flexible behaviour of the framework, is presented in Table 5.1.

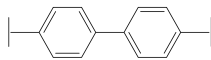
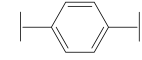
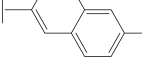
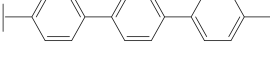
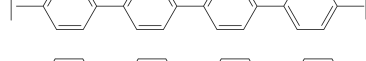
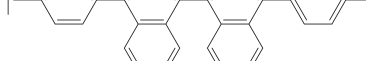
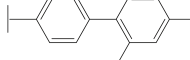
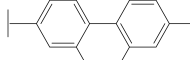
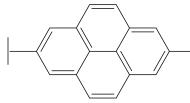
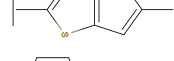
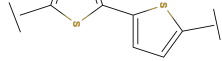
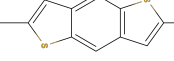
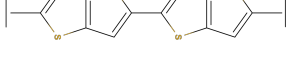
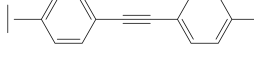
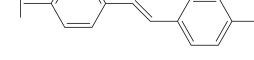
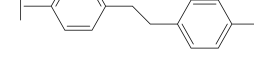
- Series dedicated to studying the influence of isoreticular design through variation of linker length in the order of theoretical increasing porosity: DUT-48, DUT-46, DUT-49, DUT-50, DUT-151/DUT-152. These materials are designed with a linker of increasing size by using differently structured phenyl rings. A corresponding increase in porosity is expected, however, starting from a 4-linear phenyl chain (DUT-151), the internal voids are large enough to allow for a secondary interpenetrated network to develop. An attempt to prevent this by grafting bulky naphthalene rings was made in the synthesis of DUT-152, but the resulting structure was still found to be interpenetrated.
- Series assessing the impact of steric hindrance of the central linker bond on NGA, in the order of connectivity: DUT-49, DUT-149, DUT-148, DUT-147. The rationale behind this approach is to improve the tensile strength of the strut by the addition of sterically hindering side connections.
- Series investigating the effect of heterocycles on compliant behaviour, using thiophene as replacement for the benzene rings, in the order of increasing linker size: DUT-170, DUT-171, DUT-172, DUT-173. If interactions with the framework plays a role in NGA, the addition of potentially stronger host-guest sites.
- Series aiming to possess a progressively more labile central strut through the use of different degrees of saturation, in order of central bond hybridization: DUT-160, DUT-161, DUT-163. It was found that the removal of solvent from DUT-162 could not be performed without structure collapse. The softness of the saturated backbone lends itself to an unstable *op* state.
- Series of increasing crystallite size to study the effect of the crystal surface to volume ratio on NGA. Different sizes of DUT-49 were synthesised either through the addition of a acid modulator for obtaining large crystals or through the addition of a base to inhibit crystal growth. A series of 4 DUT-49 materials was received, of 800 nm, 1 µm, 4 µm and 10 µm average size respectively.

### 5.3.2 Characterisation methods

In order to examine the energetic components of both adsorption and NGA, the combined manometry and calorimetry setup first presented in chapter 2 was used. Ambient temperature calorimetry was conducted at 303 K with probes such as butane, propane and propylene using the step-by-step gas introduction method. The exact procedure for such an experiment can be found in section A.10 of Appendix A.

For the experiments at 77 K, a high resolution continuous introduction method was employed, using a home-made calorimeter in a diving-bell configuration, first described in the work of <sup>?</sup>. To summarize, the adsorbate is placed in a J-shaped custom designed glass cell which is then sealed with an oxybutane torch prior to evacuation and sample activation.

**Table 5.1:** Flexible materials analogous to DUT-49

Study	Name	Linker center	Pore volume (geometric)	Observations
			cm <sup>3</sup> /g	
	DUT-49		2.24	Multiple crystal sizes • DUT-49(o)-4.4 μm • DUT-49(s)-1.0 μm • DUT-49(m)-4.0 μm • DUT-49(l)-10.0 μm
Linker size	DUT-48		1.41	—
	DUT-46		1.75	—
	DUT-50		3.23	—
	DUT-151		4.36	Interpenetrated
	DUT-152		4.13	Interpenetrated
Linker stiffening	DUT-149		2.15	—
	DUT-148		2.12	—
	DUT-147		2.11	—
Heterocycle	DUT-170		1.59	—
	DUT-171		1.67	—
	DUT-172		2.06	Not measured
	DUT-173		2.70	Not measured
Strut saturation	DUT-160		2.77	—
	DUT-161		n. a.	Not measured
	DUT-162		2.72	No stable <i>op</i> state

Borosilicate glass is selected as the material of choice to prevent any thermal expansion induced leaks. The cell is then introduced into a LN<sub>2</sub>-filled dewar, through the bottom of the differential calorimeter. Good thermal equilibrium between the cell and surrounding thermopile is ensured using by using a helium blanket in the calorimetric enclosure, kept under a small positive pressure through a continuous low flow. The connection to the gas dosing system is made through a Swagelock VCR 1/4" stainless steel connection. High leak resistance and gas purity is assured by metal-to-metal interlock with a single use copper joint. Pressure is measured through the use of a double gauge assembly, a sensitive low pressure gauge (up to 2 kPa) and an ambient pressure gauge (up to 120 kPa). A sonic nozzle is used to control the flow of adsorbate into the reference volume and the cell. A separate calibration step is performed at the start of each experiment to determine the adsorbate flowrate and the dead volume before the entrance to the cell. An experiment takes between 1–4 days depending on the flowrate used. A picture of the different components of the setup can be seen in Figure 5.3.

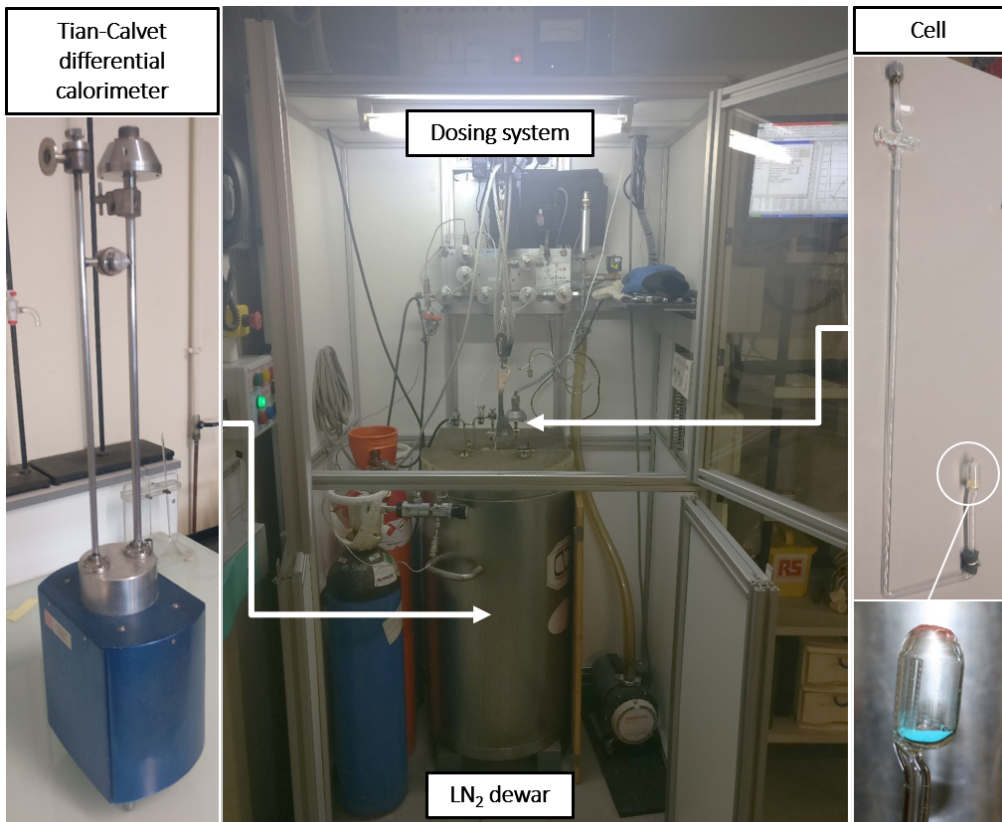


**Figure 5.3:** The low temperature calorimetry setup

Extreme care has to be taken during sample preparation, as all materials studied are sensitive to heat and water vapour, which attack the Cu paddlewheel and lead to material degradation. To prevent any decomposition, the samples were stored under an inert argon atmosphere in a glovebox. The loading of ambient temperature cells was performed inside the

glovebox while filling and sealing of low temperature glass cells was done in an argon flow. After sample cell preparation, the materials are activated under dynamic vacuum at 120 °C.

It is worth noting that if the sample undergoes an *op/cp* phase transition during the experiment and cannot be reopened with the application of high pressure, as is the case for butane at 303 K, the material cannot be reused. Any attempt to activate it under vacuum leads to structural breakdown of the unstable *cp* phase. Since a limited amount of sample is available, this played a large role in data acquisition, with several isotherms only recorded once.

## 5.4 Results and discussion

The first part of this section will present the characteristics of the NGA step in DUT-49 as recorded by ambient calorimetry, and what a cursory examination of the isotherm and enthalpy curves at 303 K can reveal about the energetics of the system and the stability of the two phases.

The following subsection contains the results of the studies on DUT-49 analogues, highlighting the effects that linker elongation and functionalization have on the adsorption behaviour and NGA extent at ambient temperature.

Finally, an in-depth study of the DUT-49 NGA mechanism is performed, employing a variety of gas probes ( $\text{N}_2$ , Ar,  $\text{O}_2$ , CO) at low temperature. The time-resolved data obtained through continuous adsorbate introduction sheds light on the influence of the host-guest and guest-guest interactions on transition mechanics, the energetic barrier of the transition state and on system kinetics. A comparison with non-flexible analogues allows an assessment of the role of the pore filling mechanism on the structural transition to be made.

### 5.4.1 The structural transition leading to NGA in DUT-49

In the time-resolved pressure and calorimetry signal recorded when performing butane adsorption at 303 K, the NGA step is clearly visible as the pressure in the cell suddenly increases after a dosing point. An example can be seen in Figure 5.4, next to a regular dosing step. A short time after the adsorbate is introduced in the measurement cell, the material contracts. The calorimeter signal is positive, therefore the overall process is still exothermic — even though desorption and structural transition, both endothermic processes, are taking place.

The signals are then processed to yield the combined isotherm and differential heat of adsorption. Figure 5.5 shows two isotherms recorded on different DUT-49 samples. Several observations can be made. First, a clear transition takes place around  $0.15 \text{ p/p}_0$ . This corresponds to the *op/cp* transition which *decreases* the amount adsorbed per gram of material. After NGA, the material is in its *cp* form, where it remains throughout the remainder of the

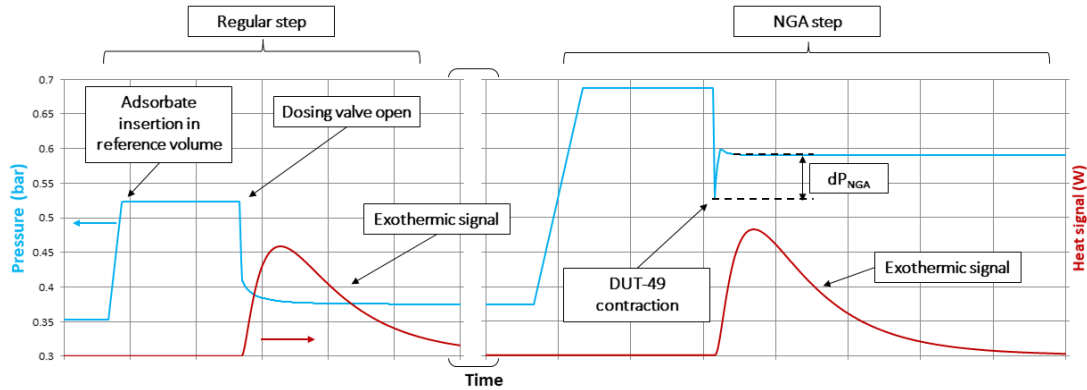


**Figure 5.4:** The pressure and calorimeter signal from butane adsorption on DUT-49, highlighting a typical step (left) and the observed NGA step (right)

measurement. Unlike in the methane experiments performed at 111 K, the structure does not re-open. A secondary transition to the *op* form is expected at higher pressures, close to the saturation pressure of the adsorbate. However, this pressure range could not be reached within the experimental conditions.

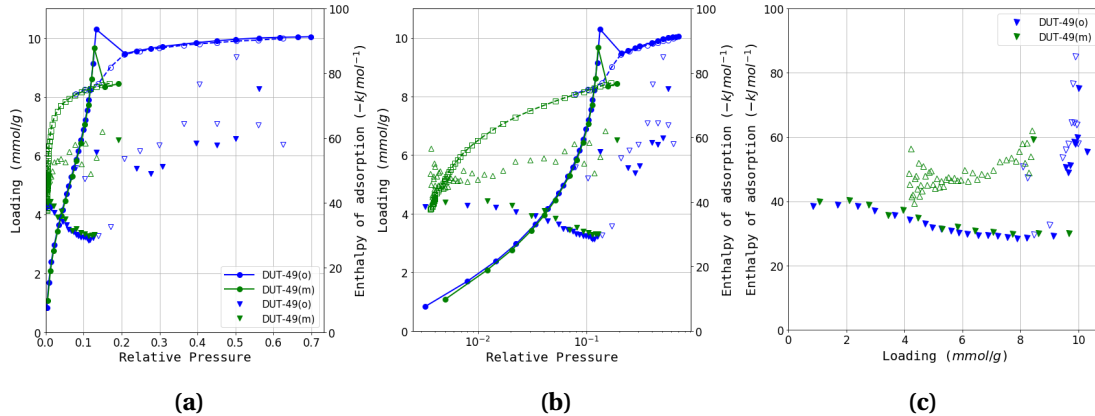


**Figure 5.5:** Butane adsorption experiments on two samples of DUT-49, DUT-49(o) and DUT-49(m) shown as (a) regular isotherms (b) logarithmic isotherms and (c) enthalpy as a function of pressure.

Due to the steep knee in the adsorption/desorption branch of the *cp* form, a complete desorption branch cannot be obtained, with the minimum attained loading of 4 mmol. As such, framework collapse is not seen in the experiments. Another shortcoming is that the isotherm and energy landscape of the *op* form in its metastable region is inaccessible, since by definition the material will undergo a transition in this pressure range.

A key feature visible in the two recorded isotherms is that, while adsorption on the open pore form fully overlaps between the two experiments, both the location and extent of NGA differ slightly. In the DUT-49(o) isotherm, a smaller NGA step occurs, with the resulting structural contraction apparently unable to achieve a complete closing of the pores. Upon des-

orption, a secondary step occurs in the same  $0.15 - 0.2 \frac{p}{p_0}$  pressure range, after which the material is fully in its *cp* state, as evidenced by the overlap with the DUT-49(m) isotherm. The reason behind the dissimilar behaviour is the contribution of crystal size to the energy barrier of transition. A thorough analysis can be found in the paper published by <sup>2)</sup> where it shown that a high surface to volume ratio has a negative impact on NGA, with smaller crystallites unable to achieve a complete contraction, instead accessing an intermediated or *ip*, with the “*a*” lattice parameter 5–7% smaller than the *op* phase rather than 24% in the *cp* phase.

The enthalpy curves in Figure 5.5c, paint a picture of the energetic landscape of both phases. First it should be noted that the differential enthalpy of the NGA step itself does not appear on the graph as it is a negative value. This is not because the transition step is endothermic, as proven in Figure 5.4. However, as the net change in adsorbed amount between the two points where the transition occurs is negative, the calculated enthalpy *per mole of gas adsorbed* takes the same sign.

In the adsorption branch, the initial enthalpy of adsorption can be observed to be around  $38 \text{ kJ mol}^{-1}$  to  $40 \text{ kJ mol}^{-1}$ . This value is higher than observed for butane in HKUST-1 in the order of  $35.6 \text{ kJ mol}^{-1}$ <sup>(?)</sup> though smaller than in another similar copper paddlewheel flexible MOF ( $50 \text{ kJ mol}^{-1}$ )<sup>(?)</sup>, and suggest that the interaction of the pore wall with the adsorbate is relatively low, probably due to the large pore size. After  $2 \text{ mmol g}^{-1}$ , the enthalpy curve slopes downwards until a local minima around  $30 \text{ kJ mol}^{-1}$  before NGA. This can be assumed to be the multilayer adsorption region, where the field gradient of the pore wall decreases and guest-guest interactions dominate. The enthalpy calculated for the desorption curve is essentially the differential enthalpy of adsorption of butane on the *cp* form. A large difference, in the range of  $10 \text{ kJ mol}^{-1}$  to  $20 \text{ kJ mol}^{-1}$ , exists between the enthalpy of adsorption in the two states. This can be attributed to the more confined nature of the *cp* form, with the smaller pore walls increasing the interaction of the framework backbone with an adsorbate molecule. The energy required to drive the transition and generate the observed thermal effect can be accounted for by the increased total interactions of remaining adsorbed molecules with the *cp* state of the framework. A more in-depth analysis of the NGA energetics will be presented in subsection 5.4.3.

### A brief mention of measurement uncertainty

In order to assess whether results obtained through calorimetry are within acceptable accuracy, uncertainty calculations have been carried out. The method used here is laid out by the International Organisation for Standardisation (ISO) in the Guide to the expression of Uncertainty in Measurements (GUM). The method is fully detailed in Appendix C, and consists of an identification of all variables used in the calculation of the final result, and estimation of the uncertainty in the final value as a function of the uncertainty in each such variable. The result is multiplied by a factor of confidence, which has been chosen as 95% in the figures

presented in Figure 5.6.

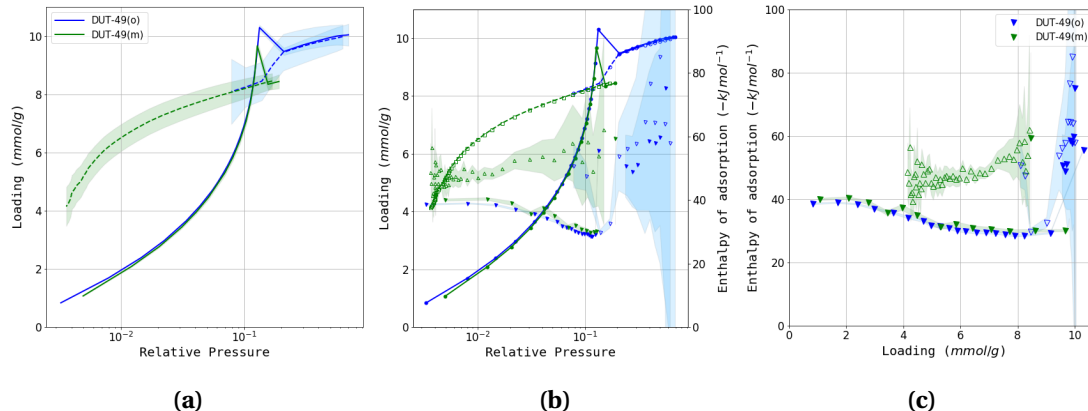


**Figure 5.6:** Estimated errors at a 95% confidence range for (a) loading as a function of pressure, (b) differential enthalpy as a function of pressure (c) differential enthalpy as a function of loading.

The use of the manometric method for isotherm measurement entails a cumulative error in the pressure measurement that leads to an increase in uncertainty with each measured point. It can be seen in Figure 5.6a that in spite of the margin of error, there is perfect overlap between the two measured isotherms in the adsorption branch and in the desorption branch. It is reasonable to assume that the error is therefore much smaller than the calculation would suggest.

The uncertainty in the differential enthalpy of adsorption (Figure 5.6b) is a function of  $\Delta n$ , the amount adsorbed in each step, as well as pressure, with the same cumulative error applicable. The former variable accounts for the large uncertainty in flat sections of the isotherm where almost no adsorption takes place, while the latter results in the spread seen at the end of the desorption curves. However, when observing  $\Delta_{ads} \dot{h}$  as a function of loading in Figure 5.6c, the uncertainty is confined to high values on the x axis, with a clear separation of isotherm branches.

As the display of uncertainty ranges clutter the isotherm graphs and makes it hard to distinguish features, the remainder of this chapter will only display them if the error range is significant.

#### 5.4.2 Impact of framework structure on transition mechanics

While the discovery of the NGA transition in DUT-49 was a result of serendipity, it opens the door to a rational design approach to modify the extent and the location of the phenomenon. In principle, there are several avenues that could be taken in order to tune the contraction mechanics.

- Changing the range of metastability of the open pore state.

- Decreasing the porosity of the closed pore state.
- Increasing the capacity of the open pore form.

These factors are bound to be tightly interlinked, with a slight alteration in one possibly leading a shift in all. For example, the addition of a stabilizing group which would increase the tensile strength of the linker is also likely to decrease the porosity of the entire system.

There are a range of physicochemical modifications available to tune the properties of the framework, many already employed in the MIL-53 and MIL-47 family of flexible MOFs. Through functionalisation or modification of the linker, the strength of the guest-guest and guest-host interactions is affected, as evidenced by the different gate opening behaviour with nitrogen and water on several functionalised versions on MIL-53.<sup>(?)</sup> In the case of DUT-49, moieties grafted to the central strut or changes in the linker backbone are also likely to affect its buckling behaviour. While the use of a different metal nodes has succeeded in changing the mechanical response of MIL-53<sup>(?)</sup>, this approach is likely to have less impact on DUT-49, as the mechanism of contraction is due to linker flexibility. A common rational design methodology is the so-called isoreticular design, where topologically isomorphic MOFs are synthesised through progressive elongation of the linker. Another path to controlling flexibility is manipulation of crystal size, as it has already been shown by <sup>(?)</sup>. Finally, structural defects, of which a description was given in chapter 3, are another degree of freedom to consider for NGA tunability. Approaches such as mixed linker synthesis and vacancy defects may allow for fine-grain influence of framework stiffness.

### Behaviour of isoreticular materials

The series of materials DUT-48, DUT-46, DUT-49, DUT-50 and DUT-151/DUT-152 was synthesised with the aim of studying the effect of linker elongation on the NGA step. It was found that the tetra-phenyl chain in DUT-151 increased the pore size to the threshold where a secondary net can form in the intracrystal voids, resulting in two identical interpenetrated frameworks. An attempt to introduce a bulky side-functionalisation in DUT-152 resulted in a similarly interpenetrated material. Figure 5.7 shows the butane adsorption dataset recorded on the non-interpenetrated versions.

Indeed, the results follow a predictable trend. First, it is worth noting that, as seen in Figure 5.7a, only DUT-49 and DUT-50 undergo an *op/cp* transition. This confirms that a shorter linker imparts the resulting MOF with a more stable backbone, raising the strain required in order to collapse the framework. The desorption branch of the non-flexible materials completely overlaps the adsorption branch in both isotherm and enthalpy, further confirming the small error in measurement (available in Figure G.1a). With an increase of linker size, a larger pore volume and consequently a higher amount of butane can be adsorbed in the open pore form. The increase in pore size is also responsible for a shift in the partial pressure

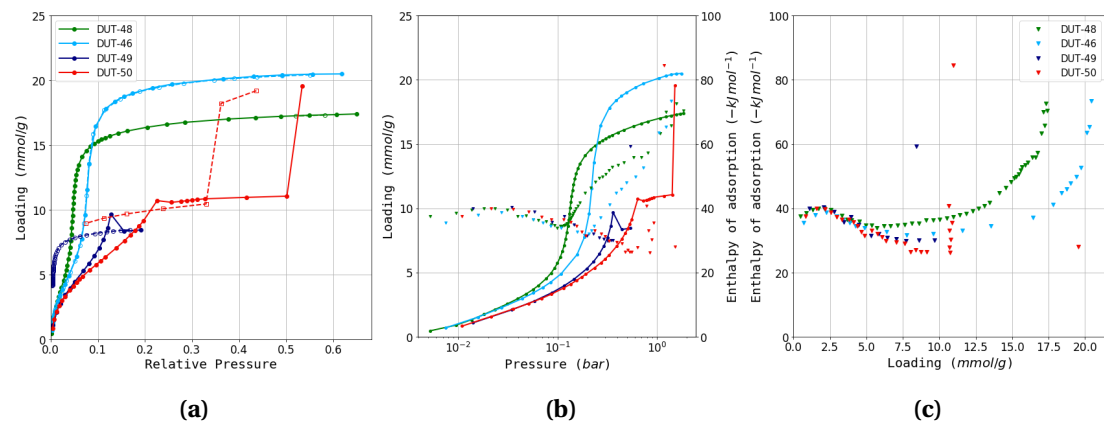


**Figure 5.7:** (a) Experimental adsorption isotherms for DUT-48, DUT-46, DUT-49 and DUT-50. Enthalpy points are omitted for clarity. (b) A logarithmic plot of isotherms and enthalpy curves, to highlight the low pressure region. (c) Differential enthalpy of adsorption as a function of loading.

corresponding to the condensation or pore filling step.

In DUT-50, the structure is seen to re-open around  $0.5 p/p_0$ , although the pressure is not high enough to completely transition to the *op* form. The collapse to the closed phase in the desorption branch achieves a lower plateau than in the adsorption branch, suggesting an incomplete *op/cp* transition as seen in one of the isotherms on DUT-49 with the smaller crystal size in the previous section.

One surprising finding is that the enthalpy curves (Figure 5.7c) present a near identical behaviour and differential enthalpy of adsorption in the low pressure region, characterized by a slight increase up to  $40 \text{ kJ mol}^{-1}$  followed by a drop-off. The adsorption mechanism and surface characteristics are therefore *common* to all four materials. The shift of the enthalpies of adsorption to lower values at higher loadings from DUT-46 to 50 is expected, with the increase in pore size leading to a progressive decrease of the contribution of dispersion interactions with the guest, which could also be referred to as a confinement effect. The steep uptake in the isotherm is indicative of a cooperative adsorption mechanism similar to a fluid condensation, accompanied by an increase in the contribution of guest-guest interactions to  $\Delta_{ads} h$ .

As neither DUT-48 and DUT-46 show any phase transition with butane at this temperature, the question arises whether their frameworks can still undergo a structural contraction. A combined simulation and mechanical pressure study was performed on DUT-48 in parallel to the microcalorimetry experiments, which can be found in the paper published in collaboration with the TU Dresden, Chimie ParisTech and ICGM groups.<sup>(?)</sup> In brief, DFT optimisations of a single linker molecule under increasing stress show that buckling of the molecule is still possible, albeit at a much higher stress. Constant volume (N, V, T) molecular dynamics simulations of the evolution of the system free energy with decreasing unit cell volume

have shown that, while a *cp* phase for DUT-48 exists, the increased tensile strength of the central backbone leads to an increase in both the free energy of this state and the activation energy required to enter it compared to DUT-49. To prove that structural transition can still take place, mercury intrusion experiments are carried out on both DUT-48 and DUT-49. The intrusion/extrusion curves on both materials show that an *op/cp* transition takes place, although with a much higher external pressure in the case of DUT-48 (65 MPa vs. 35 MPa). A similar approach on all other materials in this series reveals a very clear trend in both energy of the *cp* form and pressure required for the transition.

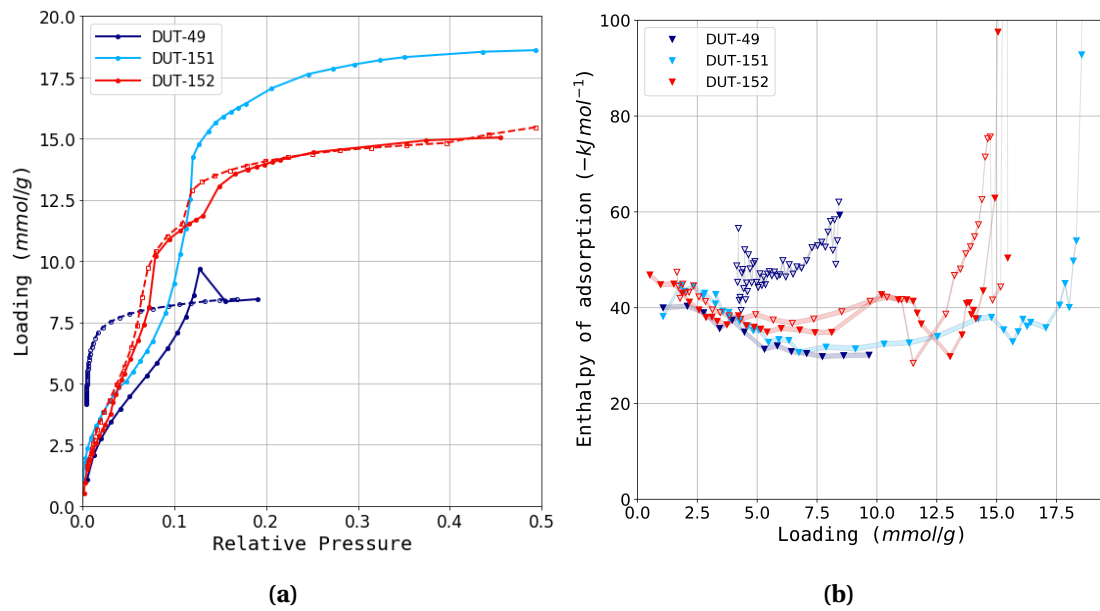


**Figure 5.8:** The (a) isotherms and (b) enthalpy curves of the interpenetrated materials DUT-151 and DUT-152 as compared to DUT-49. Shaded regions are guides for the eye rather than uncertainty domains.

The interpenetrated materials DUT-151 and DUT-152 show a very different isotherm shape and enthalpy curve, as presented in Figure 5.8. In their case, the adsorption behaviour is very complex, with multiple transitions and hysteresis loops visible. However, several trends can still be rationalized. The total pore volume of DUT-152 is lower than that of DUT-151, as the bulkier central strut lowers the available space. Both materials show steeper adsorption curves at low pressures, due to the increased interactions of the adsorbate molecules with the doubled framework net. This is reflected in the differential adsorption enthalpy in the same region, with both DUT-151 and 152 displaying a higher enthalpy ( $45 \text{ kJ mol}^{-1}$  to  $50 \text{ kJ mol}^{-1}$  as opposed to  $40 \text{ kJ mol}^{-1}$  for DUT-49). The smaller pore size of DUT-152 also leads to a shift in the adsorption isotherm to lower pressures and an increased enthalpy of adsorption at higher loadings. Finally, a total of three hysteresis loops are visible on DUT-152 associated with apparent transitions, highlighting several accessible intermediate pore states in its structure. These transitions are also found in the enthalpy curve, a result of different energetic contributions of the contraction/expansion. In order to elucidate such a complex interplay of

factors more powerful methods such as *in-situ* PXRD are required to monitor the change of structural parameters during adsorption. While interesting, it should be pointed out that all transitions on DUT-151 and 152 seem to be continuous phase changes, with no potential for an NGA-type contraction.

### Behaviour of “reinforced” linker analogues

A series of DUT-49 analogues, DUT-149, DUT-148 and DUT-147, with progressively connected central additions was created in order to observe the effect of linker strengthening on the structural transition as previously mentioned in Table 5.1. DUT-149 has two methyl groups in the ortho position relative to the central bond. DUT-148 has the same carbon number, but connects the two methyl groups with a single bond. Finally DUT-147 has a fully aromatic structure, with delocalised double bonds on each side of the original phenyl ring. The resulting isotherm and enthalpy curve are shown in Figure 5.9.

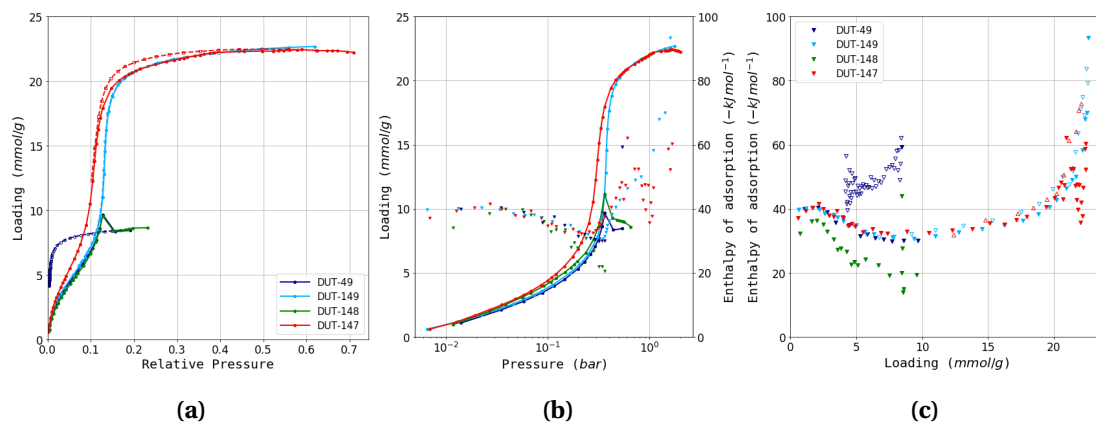


**Figure 5.9:** (a) Experimental adsorption isotherms for DUT-49, DUT-149, DUT-148 and DUT-147. Enthalpy points are omitted for clarity. (b) A logarithmic plot of isotherms and enthalpy curves, to highlight the low pressure region. (c) Differential enthalpy of adsorption as a function of loading.

An unexpected trend emerges from the measured isotherms. DUT-149 does not show an NGA step, with adsorption taking place entirely on the *op* form of the material. In this regard it is an almost perfect non-flexible variant of DUT-49, with near-complete overlap of both its isotherm and enthalpy curves. A minute shift to lower pressure can be seen in the isotherm, as the methyl groups introduce a slight decrease in the large octahedral and medium tetrahedral pore size. Counterintuitively, the next material in the series, DUT-148, undergoes structural contraction in the same manner as DUT-49, retaining the NGA transition despite its increased connectivity. Finally, DUT-147 is stiffer and maintains its *op* state throughout adsorption. A wide hysteresis appears in the desorption branch, which may be an indication of subtle structural effects such as a rotation of the central part of the linker.

The different behaviour these analogues may have two possible causes: a change in the

stability of the *cp* phase or a difference in the strain necessary to induce ligand buckling. Both parameters are influenced by the introduced functionalisations. In the case of DUT-147 the central phenyl-phenyl bond has been strengthened, resulting in an increased strain required to induce the transition and a structural failure likely taking place in the phenyl-nitrogen bonds rather than the central strut. For DUT-148 and DUT-149 the source of the counterintuitive trend is less clear-cut. In DUT-149, the methyl groups are sterically hindered, which results in the likely adoption of the lowest energy state, with the two phenyl rings at a 180° angle with each other and 90° degree with the terminal ligand planes. This steric hindrance may increase the required strain to enter the elastic buckling regime. Conversely, the single bond in DUT-148 restricts the alkyl chain to a single side of the bond and may actually lower the energetic barrier for the existence of the *cp* form, through the stabilisation afforded by a chair-like 6-ring conformer, a possible variant of which can be seen in Figure 5.10. DFT optimisations, as those performed on the previous isoreticular linkers are recommended to shed light on the buckling behaviour.

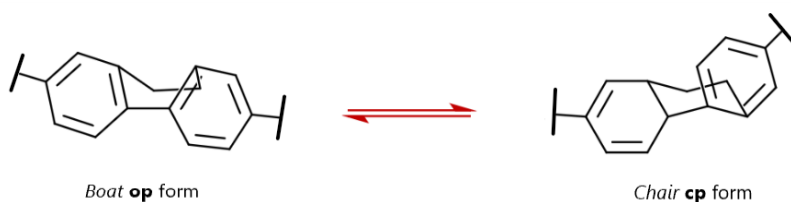


**Figure 5.10:** A possible mechanism for a conformer stabilised *op/cp* transition for DUT-148.

### Behaviour of heterocyclic DUT-49 analogues

Using a thiophene-substituted aromatic linker may introduce additional guest-host interactions due to the resulting heterogeneous pore surface. Additionally, the change in geometry allows for new flexibility modes. The butane isotherms measured on these materials are summarized in Figure 5.11.

DUT-170, which has a linker with a similar structure and length as the naphtyl-derived DUT-48 is expected to remain non-flexible. This is seen to be the case, with the two isotherms similar in regard to total amount adsorbed and pore filling pressure. The isotherm of DUT-171 does show a structural transition, but without any observed NGA. A slight hysteresis can be seen, likely due to partial structure re-opening before the beginning of the desorption branch. Instead of NGA, the enthalpy curve reveals a significant departure from the baseline as the slope of the isotherm changes slowly in a manner indicative of continuous contraction to a *cp* form. The resulting phase has enthalpies of desorption in the same range as DUT-49*cp*. This type of continuous phase change may suggest a different ligand deformation mechanism, without a sudden buckling and more akin to an elastic bending regime, perhaps due to the starting zig-zag shape of the linker.

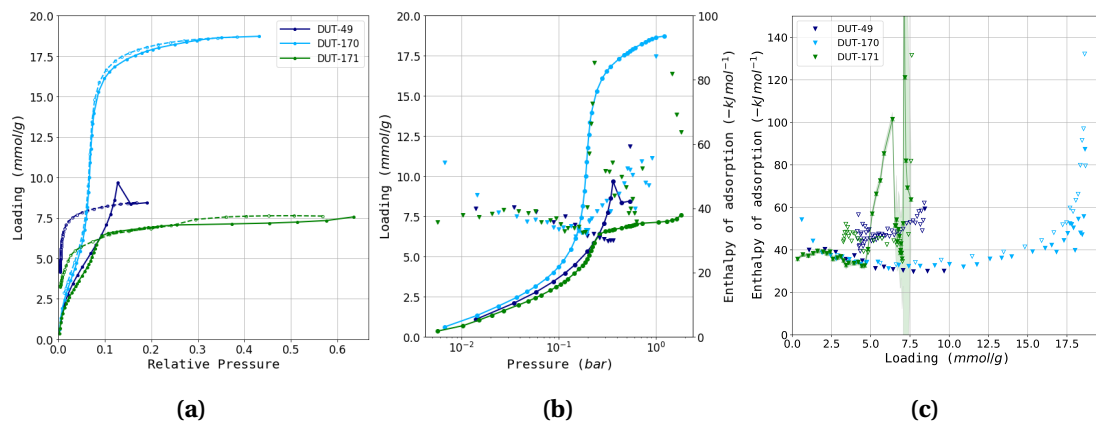


**Figure 5.11:** (a) Experimental adsorption isotherms for DUT-49 and heterocyclic analogues DUT-170 and DUT-171. Enthalpy points are omitted for clarity. (b) A logarithmic plot of isotherms and enthalpy curves to highlight the low pressure region. (c) Differential enthalpy of adsorption as a function of loading, highlighting the adsorption branch and error range of DUT-171.

Finally, the low pressure region of the enthalpy curve for DUT-170 shows a higher differential enthalpy of adsorption. However, a repeat of the experiment found that instead of a specific interaction of the heterocycle with the guest, this anomaly is due to poor thermal equilibration of the sample cell before the start of data recording in that particular measurement.

### Behaviour of elongated central strut materials

The final series of synthesised materials comprise DUT-160, 161 and 162, (Table 5.1) materials with a triple, double and single bond inserted between the central phenyl rings. In particular the behaviour of DUT-161 could prove interesting, as the linker may exist in either a *trans* or *cis* isomer. Unfortunately, DUT-162 cannot be obtained in a desolvated open pore form, as it immediately collapses upon supercritical activation. Furthermore, the yield of DUT-160 and 161 was so low that not enough material was available for an experiment with DUT-161, and resulted in large errors in the enthalpy curve of DUT-160. The recorded isotherms are presented in Figure 5.12.

From its isotherm slope change in Figure 5.12a, DUT-160 can be seen to undergo a sharp transition at  $0.2 p/p_0$ , without NGA. The isotherm is very similar to the one measured on DUT-50, whose linker is comparable in length, pointing to a similar buckling behaviour. The lack of NGA is likely due to a lower energetic barrier between the *op* and *cp* state. The enthalpy curve of both DUT-160 and 50 has the same shape, although the differential enthalpy of adsorption on DUT-160 is lower across the entire loading range, which may be a consequence of the larger uncertainty in the measurement.

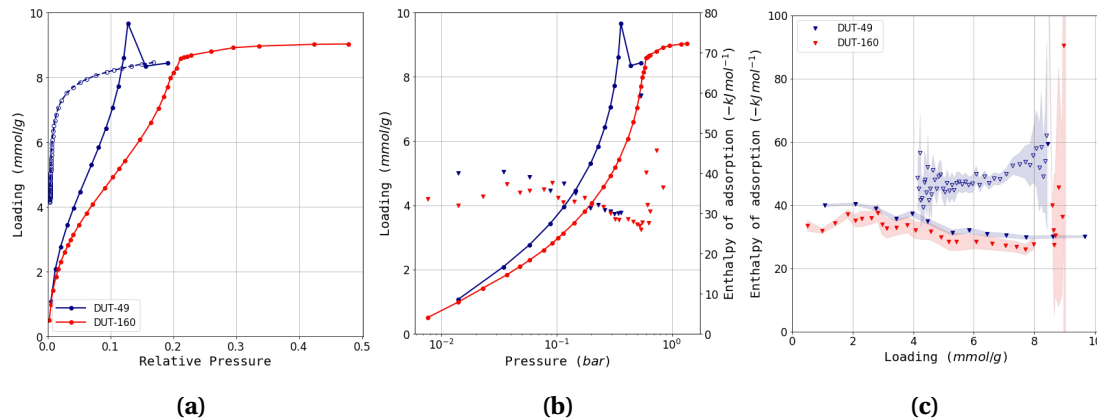


**Figure 5.12:** (a) Experimental adsorption isotherms for DUT-49 and DUT-160. Enthalpy points are omitted for clarity. (b) A logarithmic plot of isotherms and enthalpy curves, to highlight the low pressure region. (c) Differential enthalpy of adsorption as a function of loading together with the uncertainty range for each measurement.

### Overview of NGA tuning through framework modification

This extensive study of different DUT-49 derivatives demonstrates the large range of options available for tuning structural transitions in the prototypical NGA material. Both linker shortening and functionalisation lead to increased framework stiffness, in an analogue fashion to increasing the structural integrity of a pillar. This approach might allow for the design of materials which would only undergo an *op/cp* transition with desired adsorbates and temperature ranges, or limit structural collapse to mechanical pressure. The porosity limit at which net interpenetration begins to occur is found around the length of the DUT-151 linker, or 4 phenyl rings between terminal moieties, a process which does not completely suppress flexibility. More importantly, more fundamental changes to the type of flexibility, such as a continuous “breathing” phase transition, or light-induced switchability might be induced with careful choice of linker, as seen in DUT-171 and suspected in DUT-161, respectively.

#### 5.4.3 An in-depth analysis of the NGA mechanism

As it has been shown in the previous section, there are several avenues to achieve tuning of NGA in the DUT-49 framework. However, a fundamental understanding of the factors and energetics of the process may lend itself to prediction of when the phenomenon occurs without experimental input, and even lead to the rational design of similar materials.

To this end, the adsorption of multiple probes was investigated at 77 K with *in situ* continuous low temperature microcalorimetry, in order to observe the influence of the guest on the mechanism of adsorption and NGA. To obtain a baseline of adsorption in the *op* phase, a non-flexible alternative is used. DUT-149 is the most similar material out of all previously

studied analogues, as it has the same linker length and nearly identical pore size and surface area.

Four gas probes were used, chosen as they have a non-trivial saturation pressure at this temperature: Ar, N<sub>2</sub>, CO and O<sub>2</sub>. Argon, as a noble gas, has a completely spherical molecule, which does not induce any specific host-guest or guest-guest interactions. Nitrogen is commonly used as the probe in material characterisation, and carries a weak quadrupole. Carbon monoxide has been used as it often forms coordination bonds through electron donation, as well as being a weak dipole and quadrupole. Finally oxygen has a weaker quadrupolar moment than nitrogen, and can interact with the surface in a similar way. It is worth noting that both argon and carbon monoxide are below their freezing point at this temperature. A table with relevant properties of the probes used at the experimental conditions can be found in section G.1.

## Results and initial observations

A large dataset was gathered on these materials as experiments were performed with different amounts of sample, different gas introduction flowrates, as well as repeats with identical conditions to ensure that factors such as equilibrium or diffusion do not play a role in the results. No desorption isotherms can be recorded using this method, which results in an inability to obtain an enthalpy curve corresponding to the *cp* form at low pressure. A list of experiments, as well as all isotherms and enthalpy curves measured can be found in Appendix G.

Selected isotherms and corresponding enthalpy curves for both DUT-49 and DUT-149 are shown in Figure 5.13 for N<sub>2</sub> and CO and in Figure 5.14 for Ar and O<sub>2</sub>. A cursory observation of the isotherms reveals that the DUT-149 framework is not as stiff as previously assumed. A clear NGA step can be found in the oxygen isotherm, suggesting that adsorption of this probe is capable of overcoming the higher energy barrier of linker buckling in this methyl functionalised version. If comparing the isotherms measured on the two materials, they are seen to be nearly identical until structural contraction. The total amount adsorbed after pore re-opening is also in a 2% range with all probes. The assumption that the mechanism of adsorption in DUT-49 can be likened to its functionalised version holds in this case.

Another surprising behaviour can be seen in the nitrogen isotherm on DUT-49. While an NGA discontinuity is still present, structural re-opening takes place in several distinct steps, each accompanied by a sharp peak in the enthalpy curve. This behaviour is in agreement with the study published by <sup>2)</sup> on the evolution of the contraction step with variation of crystallite size. In their paper, the increase of average crystal dimensions is seen to change the material from non-flexible to a progressively better defined NGA transition. *In situ* PXRD shows that between complete structural stiffness and a purely *op/cp* phase transition, several intermediate pore forms can be accessed.<sup>(?)</sup> It can therefore be theorised that nitrogen

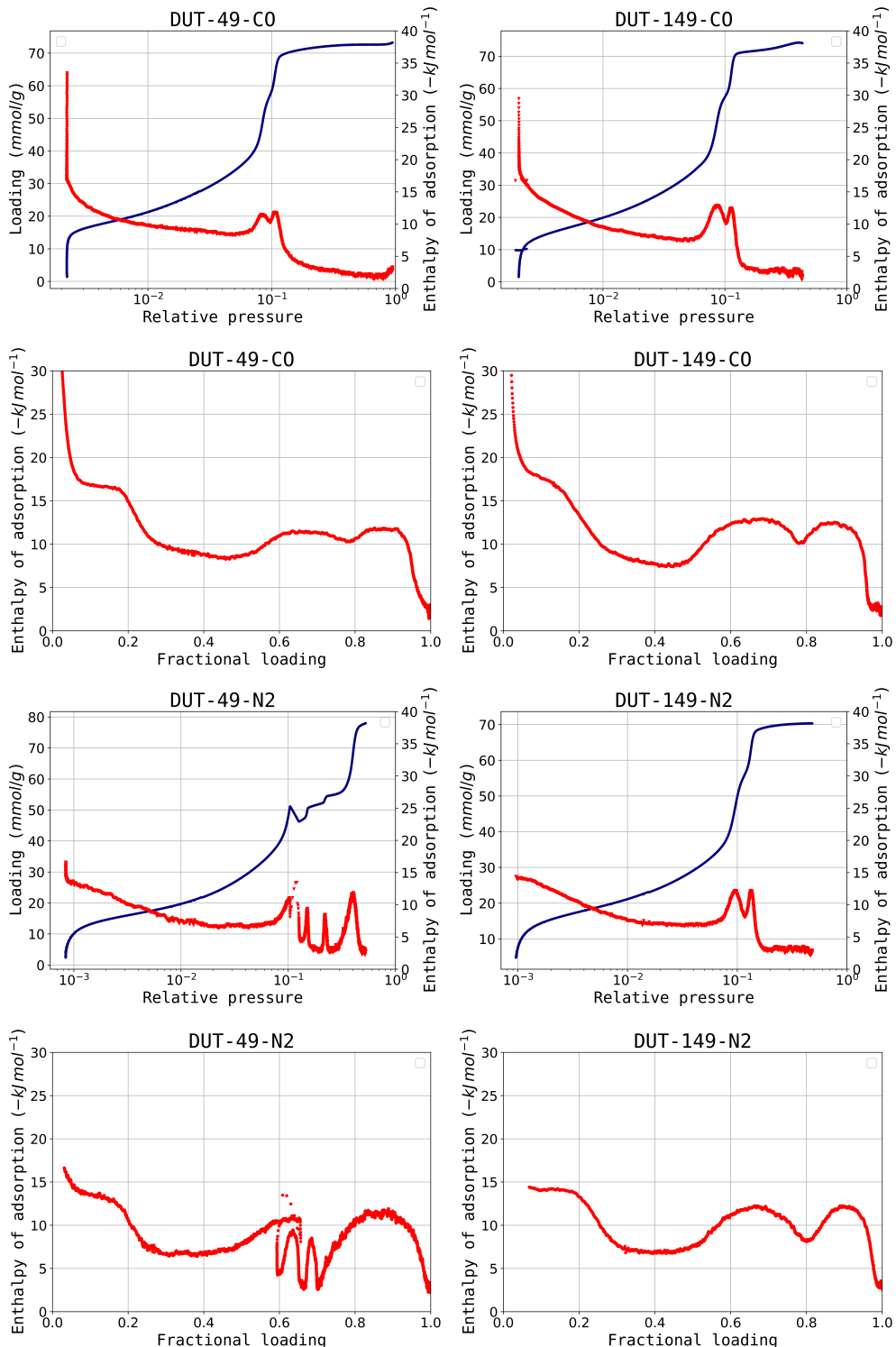


**Figure 5.13:** Carbon monoxide (top) and nitrogen (bottom) isotherms and enthalpy curves measured on DUT-49 (left) and DUT-149 (right).

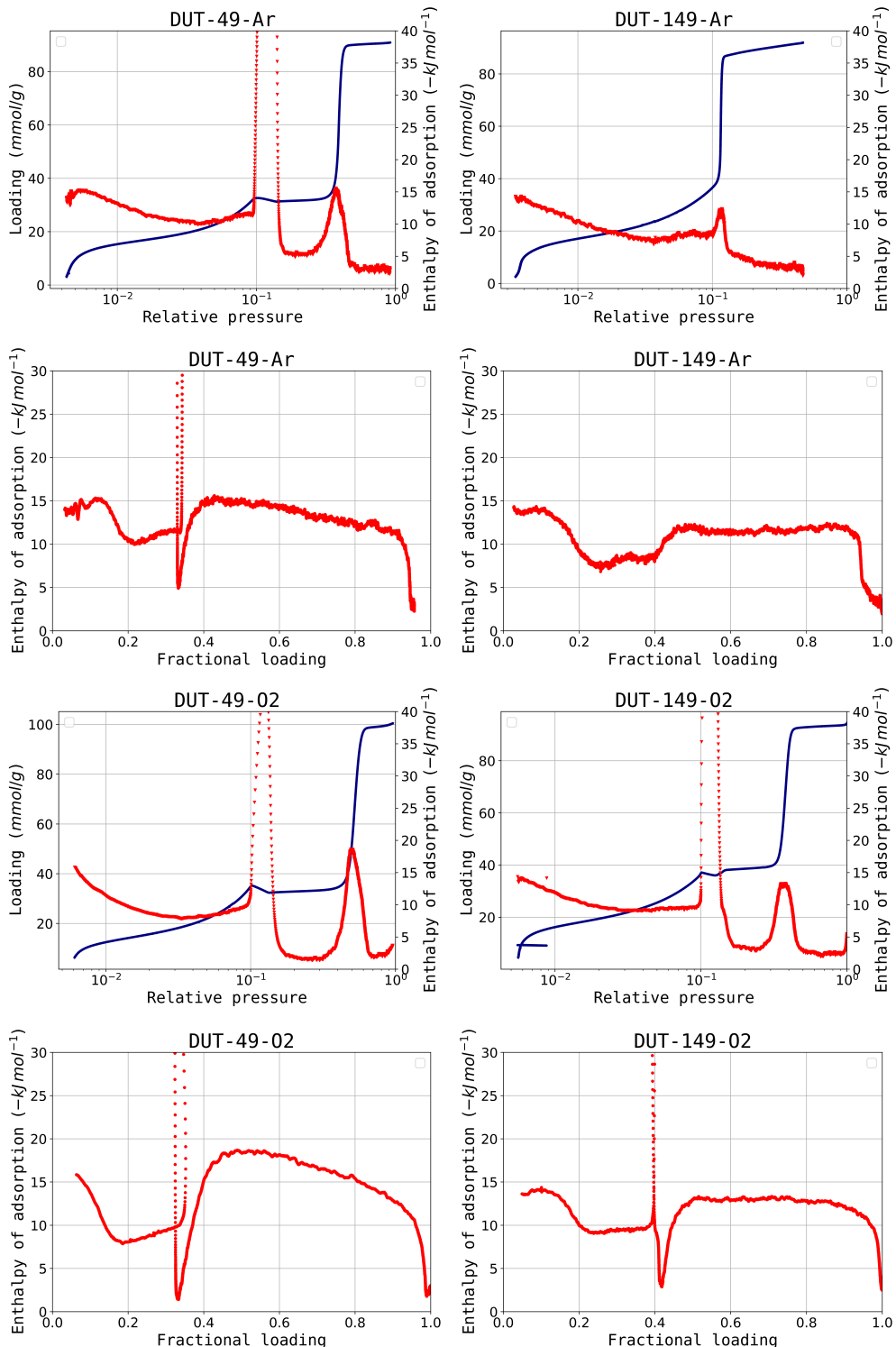


**Figure 5.14:** Argon (top) and oxygen (bottom) isotherms and enthalpy curves measured on DUT-49 (left) and DUT-149 (right).

adsorption takes place near the lower limit of favourable transition energetics, where particulate surface effects can have a high influence on the stability domain of the open pore form.

### Physical state of the adsorbate in the material pores

As two of the four gas probes are below their respective freezing point at experimental conditions, a question arises about the state of the adsorbate in the pores of the material. While a structuring of the fluid similar to a solid phase is possible inside the pores of various adsorbents<sup>(?)</sup>, it is often assumed that the adsorbed phase is more similar to a liquid, even at low temperatures.

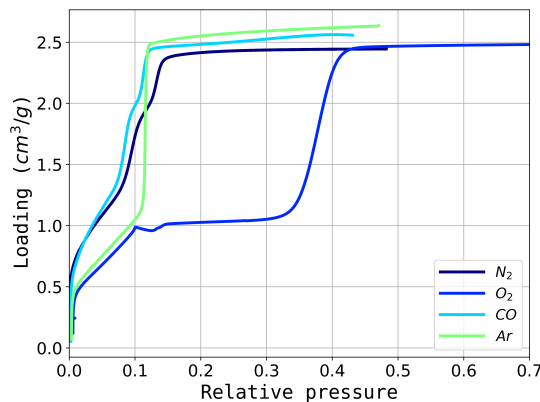


**Figure 5.15:** Volumetric adsorption isotherms of all probe gasses on DUT-149. The density of the adsorbate was obtained from a liquid phase at the corresponding temperature. It is assumed that the structure re-opening after oxygen adsorption is complete.

A simple method to check whether the phase of all measured probes is close to a liquid state, assuming that the accessible void space is identical with all probes, is to compare the total pore volume for each fluid as determined by converting the isotherm to a volumetric rather than molar basis for the adsorbate. The density used for this conversion can be either taken as the liquid density of the saturated liquid or the density of the solid phase. Figure 5.15 plots isotherms measured on DUT-149 transformed using the *liquid density*. All isotherms reach a plateau at around  $2.5 \text{ cm}^3/\text{g}$ , confirming that the fluid in the pores can be considered in a liquid state.

### Specific guest-host interactions

A common feature to almost all measured isotherms on the DUT-49 systems is the equivalent adsorption mechanism before structural transition takes place. Indeed if enthalpy curves recorded with different adsorbates at different temperatures below the critical point of the

fluid are compared at low loading, they may be mistaken for the same datapoints shifted to various enthalpy values. In adsorption in the *op* state, this “typical” enthalpy curve first increases to a local maxima, followed by a gentle downward slope. The pore filling step (or steps) are accompanied by an increase in  $\Delta_{ads} h$ , an indication of high guest-guest interactions. It is in this pore filling step where the structural contraction occurs. This prototypical enthalpy profile of the *op* phase is also seen on almost all the DUT-49 analogues in subsection 5.4.2, suggesting that it is a consequence of the topology of this structure. These features suggest that specific interactions with the framework are generally low. The only exception to this case are adsorbates which can interact with the Cu paddlewheel, either through adduct formation, electron donation or  $\pi$  backbonding interactions.

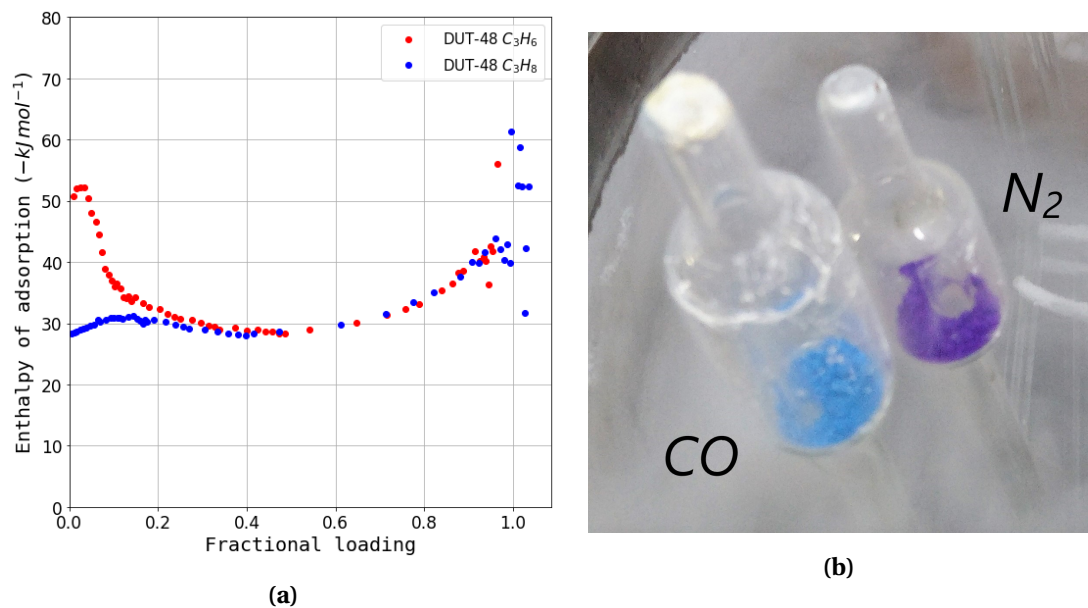


**Figure 5.16:** (a) Enthalpy curves of propane and propylene on DUT-48 as a function of fractional loading, with higher enthalpy of adsorption of the unsaturated hydrocarbon at low loading as an indication of  $\pi$ -Cu interactions. (b) Photo of DUT-149 cells filled with CO and  $\text{N}_2$  at 77 K. Note the colour change of the CO-filled cell as evidence of the formation of Cu(II)...CO adducts.

Such effects are noticeable in the CO adsorption isotherms, as the initial measured differential enthalpy of adsorption is around  $40 \text{ kJ mol}^{-1}$ , consistent with the formation of Cu(II)...CO adducts as seen in similar paddlewheel based MOF such as HKUST-1.<sup>(?)</sup> Indeed, a visual examination of the carbon monoxide saturated DUT-149 at 77 K (Figure 5.16b) shows a pronounced colour shift and suggests a change in the coordination sphere of the copper atoms. As the sample is brought to ambient temperature, the cyan colour disappears, attesting that there is no strong coordination bond, such as is typical in more stable Cu(I)...CO coordination compounds.

A separate study on the possible interaction of  $\pi$  bond containing unsaturated hydrocarbons was performed using ambient temperature calorimetry. Propane and propylene isotherms

and enthalpy curves were recorded on the shorter linker, non-flexible DUT-48. Figure 5.16a reveals that there is indeed a larger enthalpy of adsorption at low loadings when propylene is used as the probe gas, with the curves overlapping after the initial region. The difference of around  $20 \text{ kJ mol}^{-1}$  between the two initial enthalpies of adsorption is consistent to what has been predicted and recorded on the copper center in HKUST-1<sup>(?)</sup>, and can be explained through the formation of a partial dative bond between the propylene  $\pi$  orbital and the  $\text{Cu}^{2+}$  cation.

In both the case of CO and  $\text{C}_3\text{H}_6$ , the stronger interactions occur only at fractional loadings below 0.1, before the occurrence of NGA. The enthalpy of adsorption after this region take values which are close to those of similar probes ( $\text{CO-N}_2$ ,  $\text{C}_3\text{H}_6\text{-C}_3\text{H}_8$ ). This is further evidence that, while specific guest-host interactions may exist, they play a negligible role in the mechanism of contraction.

### Pore filling mechanism of the *op* phase

If focusing on the pore filling behaviour of DUT-149, two types of mechanisms can be seen. While the initial part of the isotherm (below  $0.1 \text{ p/p}_0$ ) is typical of BET-type multilayer adsorption with a possible micropore filling step at very low pressure, the large framework pores are seen to be filled in either a single or two-step process. Both nitrogen and carbon monoxide have two distinct filling steps, which seem to correspond to the octahedral and tetrahedral pores, respectively. The two steps are accompanied by identical peaks in the enthalpy curve. This points to a similar filling process for both pores, with cooperative adsorption dominating the pore filling mechanism rather than guest-host effects. The argon isotherm, similar to the behaviour of butane at 303 K, shows a very sharp single-step process, which can be likened to condensation in a mesopore. As the two pores in the DUT-49/149 framework are interconnected through windows of  $\approx 1 \text{ nm}$ , pore filling in one type of pore can induce filling in the adjacent pore of a larger size. The sudden transition to the fluid phase can further be understood if considering the MOF pores are nearly in the mesopore range. Adsorption in such pores can be characterised through the formation of a vapour-like spinodal if the pore size is within a “critical hysteresis radius”<sup>(?)</sup>, a metastable state which subsequently undergoes a phase change when nucleation occurs. Unfortunately, the presence of a hysteresis loop cannot be confirmed, as no desorption isotherms can be obtained through the continuous method.

For a better understanding of the pore filling mechanism, adsorption in DUT-49 was studied by Krause and collaborators through *in situ* neutron powder diffraction (NPD) during adsorption of deuterated methane  $\text{CD}_4$  at 111 K, and complemented by Evans through grand canonical monte carlo (GCMC) simulations of the same system. Refinement of the NPD patterns allowed the distribution of the adsorbed  $\text{CD}_4$  in a structural unit cell to be obtained, which was further analysed using a radial distribution function to determine how the filling

of each pore as a function of pressure occurs. Results show that adsorption first takes place inside the SBU, on the copper open metal sites. Figure 5.17 reveals how the filling of each pore contributes to the overall isotherm. As expected, the SBU pore is completely filled at very low pressures and corresponds to the initial “knee” in the adsorption isotherm. Gradual pore filling then takes place until a condensation step which leads to complete filling of all pores. This step coincides with the structural transition associated with NGA and is likely a driver for the contraction.

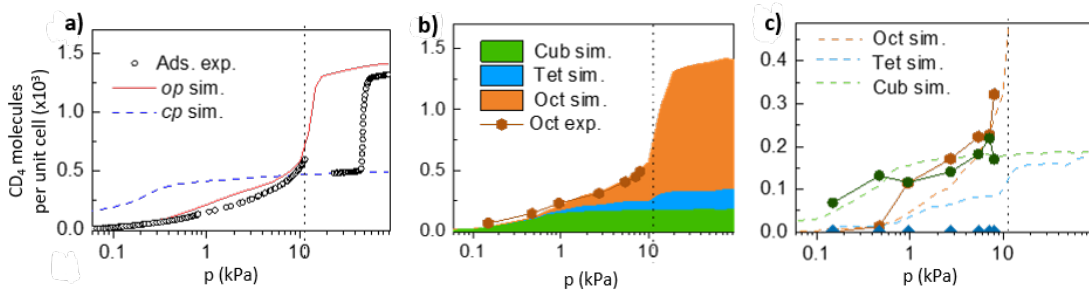


**Figure 5.17:** (a) Experimental and simulated  $\text{CD}_4$  isotherms at 111 K for *op* and *cp*. (b) Stacked simulated isotherms of different pores and experimentally obtained isotherm. (c) Comparison of simulated (dashed lines) and experimental (solid lines) for the three pores. Vertical dashed black line indicates the region of NGA.

### Relating adsorption conditions to structural contraction

As continuous adsorption introduction is a time-resolved technique, the signal obtained during the structural contraction step can be examined for clues about the energetics of transition. An example of peaks obtained during the NGA step can be observed in Figure 5.18. It is immediately obvious that the nitrogen transition is actually endothermic, unlike the signal obtained during the argon and oxygen experiments.

As the system contraction is responsible for a pressure increase in the unit cell, transition of any crystallite is likely to be a trigger of a cascade effect, where local increases in guest partial pressure induce collapse of neighbouring particles. As such, deconvolution of the calorimeter peaks during the NGA is a nearly impossible task, since minute factors such as diffusion effects, cell geometry, sample amount or flowrate can drastically change the shape of the evolved signal. However, integrating the heat recorded throughout the NGA step should give an independent value of such substeps as it represents the total heat of the transition. The average values of the observed energetics of NGA presented in Figure 5.18 paints an interesting picture regarding the influence of the adsorbate. The stress induced by the probe gas differs with its physical nature. A good indication of guest-guest interactions at a particular temperature is the enthalpy of vaporisation ( $\Delta H_{\text{vap}}$ ) of a saturated liquid. Indeed, the magnitude of the transition energy appears to be related to this value, as oxygen which has the highest

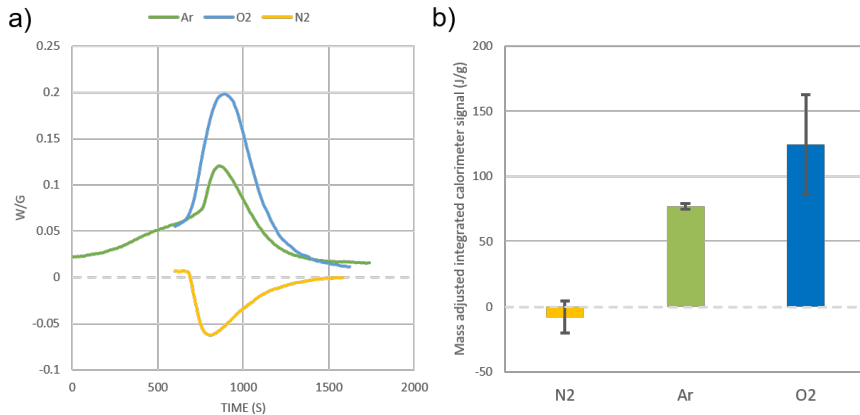


**Figure 5.18:** (a) An example of three recorded signals during structural contraction on DUT-49 with nitrogen, argon and oxygen. (b) Integrated calorimetric heat signal from nitrogen, argon and oxygen experiments. Error bars represent one standard deviation from the dataset mean.

$\Delta H_{vap}$  out of all probes used also capable of inducing transition in stiffer frameworks. By plotting the enthalpy of vaporisation for different adsorbates and adjusting it by assuming the energetic barrier is purely entropic, a remarkable correlation with the existence windows of NGA extending up to ambient temperature and with different probes can be found, as seen in Figure 5.19. This empiric model can seemingly predict the energetic limit for a favourable transition, and may be a reflection of the true energetics of the system in the subset of cases where the assumption of pure guest-guest interaction overcoming an entropic barrier holds. However, carbon monoxide is seen to deviate from the predicted behaviour and exhibit no NGA at 77 K. It could be that the increased interactions with the framework metal sites account for a larger energy barrier.

It is also worth noting that an inverse relationship exists between the exothermicity of the transition step and the amount of fluid ejected from the structure pores during the NGA step, with nitrogen experiments generating the highest  $\Delta n_{NGA}$  even if the transition to a *cp* state is incomplete. As the energy required for the expulsion of the material from the pores can be thought of as the enthalpy of desorption of the same amount from the closed pore, this component should be considered if attempting to calculate the energy difference between the two states. Repeating continuous microcalorimetry experiments at a different temperature, such as in an argon bath at 87 K, would allow for the temperature dependence of the adsorbate influence to be recorded. It is highly likely that NGA would be completely suppressed in the case of nitrogen and perhaps argon on DUT-49.

### Effect of cycling on DUT-49 transition

By increasing the partial pressure of any of the low temperature calorimetry probes over  $\approx 0.8 p/p_0$ , a re-opening of the structure can be observed. If the sample is exposed to vac-

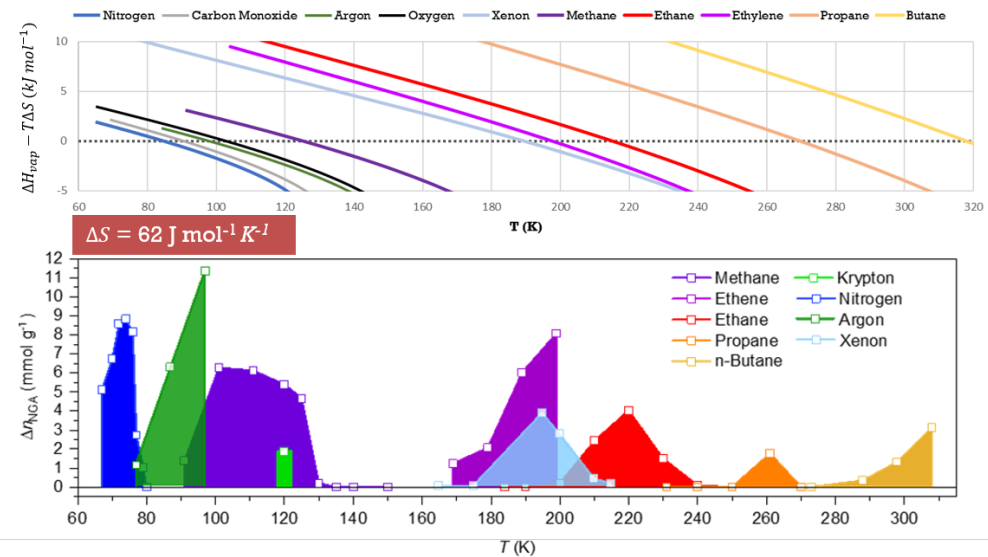


**Figure 5.19:** A surface obtained by subtracting an entropic contribution from the enthalpy of vaporisation of several common adsorbates (top) compared to the magnitude and existence region of NGA measured on DUT-49 with various adsorbates by Krause and collaborators (bottom).

uum while at 77 K, it collapses to the *cp* phase during desorption and undergoes a structural breakdown due to the instability of this form. However, if the temperature is raised above the adsorbate critical point while maintaining the sample at saturation pressure, the material can be kept in the *op* phase. No NGA has been observed with supercritical adsorbates, which is why the material is normally activated via this method.

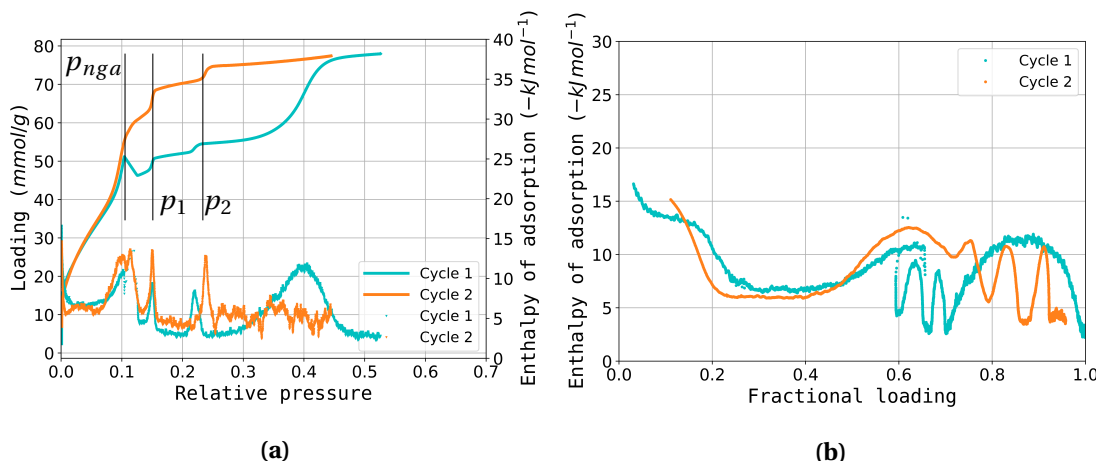


**Figure 5.20:** Isotherms (a) and (b) enthalpy curves of nitrogen on cycled DUT-49. The lines are guides for the eye.

Repeating nitrogen adsorption on a DUT-49 sample which has been cycled in this manner reveals a different kind of isotherm, as seen in Figure 5.20. While the initial part of the isotherms overlaps fully, the second experiment does not show an NGA step. Further cycling

on this cell shows only isotherm of this type. Other repeat experiments with different cells (Figure G.14) show a progressive suppression of the NGA step accompanied by an upwards shift of the plateau at  $0.3 p/p_0$ . It is likely that a structural transition still occurs in the second cycle in Figure 5.20, signalled by the small peak in the enthalpy curve at the end of the peak corresponding to the filling of the medium pore. Two progressive smaller steps can be seen in both isotherms. These may be associated with structural re-opening, but can also be due to pore filling steps in partly contracted pores. The differential enthalpy peaks corresponding to the secondary steps in the isotherm are of higher magnitude in the cycled isotherm suggesting a higher contribution from the intermediate pore phase. This effect is not seen on cycling with other adsorbents, as the NGA transition is fully developed in each cycle.

A possible explanation can be found if recalling the effect of crystal size on nitrogen induced NGA.<sup>(?)</sup> It is likely that the sample exists as a mixture of different crystallite sizes, some large enough to be capable of an NGA-type transition while smaller ones only contract to an intermediate pore state (or even remain in the *op* state). The cycling may introduce large scale defects such as dislocations or lead to the cleavage of existing grain boundaries, effectively reducing the average crystal size and increasing the percentage of material which cannot undergo complete contraction. Experimental evidence for the coexistence of both the *cp* and *op* phases after the transition pressure can be found in the  $^{129}\text{Xe}$  NMR study performed by <sup>?</sup>. In their paper, the chemical shift of  $^{129}\text{Xe}$  is monitored during adsorption at 200 K. The resulting peaks can be attributed to the two phases of the material and a small open pore signal is seen to be present concomitantly with the closed pore form. This kind of behaviour further stresses the contribution of surface potentials on the occurrence of NGA.

### **Overview of the mechanism of contraction in DUT-49**

From a structural perspective, two requirements are highlighted for NGA to occur. First, the free energy surface as a function of loading and unit cell volume must have two local minima, corresponding to the two phases of the framework. An inversion of the overall stability of the two phases must occur as the guest is loaded, which will place the system in a metastable state. While the transition is energetically favoured, the activation barrier between the two forms must be overcome, and the contraction becomes kinetically controlled. The stability of the two phases depends on the combined contribution of the framework together with the stabilisation effect of the adsorbed molecules, which can also be represented as the difference in *integral* enthalpy of adsorption between the *op* and *cp* states. On the other hand, the energy barrier between the two states can be traced to the buckling limit of the linker.

## 5.5 Conclusion

In this chapter, an extensive study of the unique phase transitions in the flexible framework of DUT-49 and its analogues was performed through combined adsorption and microcalorimetry. The results offer insight into the mechanism of phase transition and the influence of structural modifications on the contraction step, as well as corroborate the ongoing multi-pronged efforts by collaborating groups to understand this type of transition.

Exploring several approaches for tuning the NGA step through framework modification using adsorption microcalorimetry has revealed interesting findings regarding what linker properties can influence the barrier to structural transition and stability of the two phases. If a high level overview of results from different methods and groups is constructed, these properties can be generally summarised as follows.

- Stiffening of the central linker can be achieved through linker shortening or side functionalisation, usually accompanied by a reduction in total pore volume. Structural contraction may still take place through adsorption in conditions of strong guest-guest interactions or through mechanical pressure.
- Lengthening of the linker can increase porosity, but is only effective before framework interpenetration occurs, after which complete structural contraction is prevented.
- Different linker hinging systems may change the mechanism of contraction, but a ligand backbone with deformable bonds is essential for phase transition.

Extending the characterisation through microcalorimetry at 77 K with other probes allows an in-depth exploration of the guest-host and guest-guest interactions in the DUT-49 system. First, it is confirmed that under the experimental conditions, the adsorbates can be assumed to be in a liquid state in the pores. DUT-149 is selected as a non-flexible analogue, which allows for complete adsorption curves on the *op* state of the framework to be recorded, except during oxygen adsorption, when the increased energy barrier induced through linker functionalisation is also overcome. The enthalpy curves of all the probes used are seen to be similar in the low pressure region. Even in adsorbates which interact strongly with the copper atoms in the MOP, such as carbon monoxide and  $\pi$ -bond containing hydrocarbons, the increased interactions with the framework affect only the initial 10% of all adsorbed guests. Together with the location of NGA in the secondary pore filling step, guest-guest interactions are determined to be the dominant contribution to the transition mechanism. The pore filling process itself is likened to a condensation step, which is confirmed through *in situ* powder neutron diffraction results. The probes used reveal the lower limits of the DUT-49 and DUT-149 phase transitions at 77 K with nitrogen and oxygen, respectively. The calorimetric signal during the NGA step is seen to be an indication of the energy required or generated during contraction. The emerging trend of  $N_2 < Ar < O_2$  can then be related to the strength of temper-

ature and probe dependence of NGA through the enthalpy of vaporisation of the fluid.

However, many questions and research opportunities still remain about the system as a whole. From an adsorption standpoint, a rigorous theoretical model of the influence of the adsorbed phase on the forces acting on the framework is still lacking at the current time. From a material point of view, the particular molecular properties that can affect the activation barrier between the two phases without decreasing the stability of the closed pore from have only been subject of a cursory examination. Furthermore, the influence of crystal size and surface on the barrier of transition is yet to be quantified. The use of a copper paddlewheel leads to instability to humidity and it is currently not known if the metal has an influence on transition mechanics. Finally, tantalising applications, unique to such systems can be envisaged, like micromechanical switches or pressure amplifiers.

Beyond the properties of this particular framework, it is shown that the assumption of a static porous solid during adsorption can often diverge significantly from the behaviour of a real system. In particular with soft materials such as MOFs, flexibility may introduce unexpected and counterintuitive phenomena which can only be elucidated through the use of the use of complementary techniques such as *in situ* microcalorimetry, NMR, electron and neutron diffraction and advanced *in silico* simulations. The result is an exciting area of fundamental science.